



PRP-Lysate Infused Gelatin Hydrogel as a Scaffold for Bone Reconstruction

Citation

Nadra, Meral. 2019. PRP-Lysate Infused Gelatin Hydrogel as a Scaffold for Bone Reconstruction. Doctoral dissertation, Harvard School of Dental Medicine.

Permanent link

<http://nrs.harvard.edu/urn-3:HUL.InstRepos:42080545>

Terms of Use

This article was downloaded from Harvard University's DASH repository, and is made available under the terms and conditions applicable to Other Posted Material, as set forth at <http://nrs.harvard.edu/urn-3:HUL.InstRepos:dash.current.terms-of-use#LAA>

Share Your Story

The Harvard community has made this article openly available.
Please share how this access benefits you. [Submit a story](#).

[Accessibility](#)



PRP Lysate-infused Gelatin Hydrogel as a Scaffold for Bone Reconstruction

A Thesis Presented by

Meral Nadra, BDS, MDS

To

The Faculty of Medicine

In partial fulfillment of the requirements

for the degree of

Doctor of Medical Sciences

Advanced Graduate Education

Implant Dentistry

Research Mentor

Myron Spector, Ph.D.

Professor of Orthopedic Surgery(Biomaterials) Brigham and Women's

Hospital/Harvard Medical School

Harvard School of Dental Medicine

Boston Massachusetts

April 2019

This thesis is dedicated to
the love of my family
To My Mother, Father, and my two beloved sisters

Acknowledgments

First and foremost, I want to express my deepest gratitude to my research mentor Professor Myron Spector whom I wouldn't have been able to accomplish the work done in this project without.

I'm truly grateful for his enormous support, guidance and inspiration. He has always been there for me throughout all the challenges with his insightful suggestions and discussions which helped us achieve our goals. I could have never asked for a better mentor who hasn't only helped me grow professionally but also personally teaching me patience, perseverance and being a great mentor who I will always look up to.

I would like to also acknowledge my colleagues at Dr. Spector's Tissue Engineering and Regenerative Medicine Lab at the Veteran's Affairs Medical Center, JP, Boston.

Specially Dr. Wanting Niu for her help in different aspects of the project.

I would like to express my sincerest thanks and deepest appreciation to my thesis proposal committee members: Dr. Bjorn R. Olsen, Dr. Howard Howell and Dr. Giuseppe Intini in addition to the thesis defense committee Dr. German Gallucci, Dr. Yefu Li and Dr. Howard Howell for their precious time, insightful comments, valuable feedback and comments that kept me moving forward with this research. I truly appreciate their genuine advice throughout my whole work.

I would like to thank our collaborators Dr. Motoichi Kurisawa at A*STAR in Singapore for providing the Gtn-HPA conjugate to fabricate different formulations of Gtn-HPA.

Lastly but not least I would like to specially thank Dr. Ronald Baron's lab team members: Shawn Berry and Dorothy Hu for sharing their expertise and time to help me with sectioning the calcium phosphate 3D printed blocks which required dramatic modification to the protocol they do for their samples. Their valuable insights made me learn a lot on resin embedding techniques and helped me move along to different methodologies in my research.

Personal Acknowledgments

Beyond everything, I would like to utterly thank my family for their unconditional, endless love, and support in every possible way.

My beloved father Salah Nadra and My mother Manal Adam for all the sacrifices that they have made, their unparalleled love, patience, continuous encouragement that gave me the strength and faith to keep going through all the hard times.

my beloved sisters Merna Nadra and Manal Nadra, for their love, care and their exquisite ways to inspire me and keep me motivated in every step of the way.

I want to genuinely thank a dear friend of mine, Dr. Karim Elkholy who has been always there to support, help, guide and encourage me throughout the whole process.

Dr. Dominique Rousson for his continuous guidance, support and encouragement.

My dearest kind-hearted friend Zahra Aldawood for her genuine care, support, and advice.

My forever friend Noura Elbendary for her endless love and encouragement.

My closest friend and my HSDM journey companion Simon Doliveux for always being there for me.

My dear friend Marwan Cheguenni for his exceptional uplifting spirit and support.

I couldn't have asked for more genuine people in my life, I wouldn't have done it without them.

Table of contents

Abstract.....	7,8
Introduction, research background, and motivation.....	9,10
Research background and significance.....	11
Bone development, repair, and regeneration.....	12,13
Alveolar ridge healing and clinical relevance.....	14
Current grafting techniques, materials, their challenges and shortcomings.....	14,15
Tissue Engineering Triad, novel approaches and promises for the field “Tools to optimized regeneration”.....	16
Platelets and their role in healing.....	17
Growth factors and tissue repair.....	18-19
Hydrogels and their current applications in regenerative medicine therapeutics.....	20-22
Significance.....	23
Innovation.....	24
Hypotheses, specific aims and outcome measures.....	24-26
Materials and methods.....	28-39
Results.....	40-50
Discussion.....	50-53

**Future directions and preliminary qualitative assessment
results for experiments with 3D printed blocks.....54-56**

Conclusions.....56

Appendix.....56-62

Bibliography.....63-65

Abstract

Research Mentor: Myron Spector, Professor of Orthopedic Surgery(Biomaterials) Brigham and Women's Hospital/Harvard Medical School

DMSc Candidate: Meral Nadra, BDS, MDS, Advanced Graduate Education Implant Dentistry

In implant dentistry, large vertical and horizontal ridge deficiencies are challenges clinicians continue to face. Despite the current advances in grafting materials and techniques used in the clinic, often the reconstructed defect is inadequate to support implants. The complications rate for vertical alveolar ridge augmentation varies from 12% for guided bone regeneration to 24% and 47% for bone blocks and distraction osteogenesis, respectively. One of the problems related to the use of porous calcium phosphate blocks for these applications is the absence of a suitable scaffold/matrix within the pores to enable host osteogenic and vascular cells to migrate into the block, proliferate, and synthesize new bone. For smaller defects, this role is often met by the blood clot which provides a fibrin matrix and platelet-derived growth factors. For porous blocks in large defects, however, a clot does not adequately fill the pores and does not persist long enough to accommodate cell migration into the center of the block.

The **overall objective** of our work was to develop a gelatin-based gel incorporating platelet-rich plasma lysate, to mimic the role that a blood clot would normally play to attract and accommodate the migration of host osteoprogenitor and endothelial cells into the scaffold and thereby facilitating bone reconstruction. A conjugate of gelatin (Gtn) and hydroxyphenyl propionic acid (HPA) was commended for this use because of its ability to undergo enzyme-mediated covalent cross-linking under the control of horseradish peroxidase and hydrogen peroxide. **One specific aim** of this study was to assess the migration of rat mesenchymal stem cells (MSCs) into Gtn-HPA under the influence of rat platelet rich plasma (PRP) lysate incorporated into the gel. Gels incorporating PDGF-BB and without growth factor incorporation (blank gels) served as control groups. We hypothesized that the growth factors in PRP lysate would serve as chemoattractants for the MSCs. The **second specific aim** of this study was to assess the permissibility of the hydrogel of differentiation of MSCs into osteogenic cells. The hypothesis was that the incorporation of PRP lysate into the hydrogel scaffold improves bone regeneration.

One of the challenges in incorporating growth factors into biomaterials to improve the host regenerative ability is the duration and sustainability of their release at the site of the defect. The duration of release from many biomaterials is limited to a few days. This period needs to be extended for vertical and horizontal bone reconstruction. A **third specific aim** was to evaluate the growth factor release profile from the Gtn-HPA. Our hypothesis was that the Gtn-HPA will not only serve as a scaffold but also can act as a delivery vehicle that allows sustained and controlled release of the infused therapeutic agents over extended periods of time.

Results: The number of MSCs migrating into the hydrogel was significantly higher in the PRP lysate-incorporating hydrogel group (640 ± 240 ; mean \pm SD) compared to the PDGF-BB (196 ± 81) and the blank gel control groups (160 ± 41); $n=6$; p -values were 0.0006 and 0.0003, respectively.

For the differentiation/osteogenesis assay, the area% of osteocalcin +cells was significantly higher in both the gel/PRP and gel/PDGF-BB groups, compared to the two control groups. where cells in the blank gels were supplemented in one group with cell expansion medium and the other with osteogenic medium.

The results of the ELISA release assay indicated that Gtn-HPA acted as an effective delivery vehicle for the sustained release of PDGF-BB from 2 different PRP-lysate batches, with about 58%-64% of the original PDGF-BB amount in the two groups remaining in the gel at 28 days.

Conclusions: The results of the *in vitro* experiments supported our 3 hypotheses regarding the utility of Gtn-HPA for bone reconstruction. The data showed that Gtn-HPA was permissive of cell migration. PRP-lysate infused hydrogels displayed increased rat MSC migration into the Gtn-HPA compared to the blank gel. Regarding the differentiation/osteogenesis assay, the PRP-lysate and the PDGF-BB incorporating gel showed a greater area% of osteocalcin+ cells compared to the blank gel containing hydrogel. The release of the growth factors from PRP lysate, incorporated onto the gel, extended over the period of time necessary for bone reconstruction.

These findings commend Gtn-HPA incorporating PRP-lysate for infusion into porous calcium phosphate blocks for vertical and horizontal ridge reconstruction.

Keywords:

Bone grafting, tissue engineering, bone regeneration, hydrogel, Gelatin-HPA, PRP-Lysate , 3D printed Calcium phosphate porous blocks, Implant Dentistry.

Introduction, literature background, and motivation:

Dental implant therapy has proven to be of great value for treating partially and fully edentulous patients. However, following teeth extraction, alveolar ridge remodeling usually results in an inevitable vertical and/or horizontal bone loss. Adequate alveolar bone volume and adequate soft tissue are needed for proper implant placement ensuring good functional and esthetic long-term outcomes. [1] Lacking of adequate volume of alveolar bone to support implants can be due to various reasons such as previous trauma, dental infections, developmental or congenital malformations or as a sequela of periodontal disease or teeth extraction. This bone loss often leads to insufficient implant support, thereby complicating oral rehabilitation implant therapy.

There are a wide array of materials and techniques that are currently being used in the clinic for alveolar ridge augmentation.

In a systematic review by **Esposito et al. 2009** [2] the efficacy of different augmentation techniques was evaluated. The authors concluded that although there were many augmentation techniques and grafting substitutes, it's yet unclear which are the most efficient.

Attempting to overcome the complications of the current grafting procedures and the different limitations of the available grafting materials, new avenues of research are being opened using additive manufacturing methods to engineer 3D printed scaffolds aiming at improving regeneration by mimicking the microstructure and the macrostructure of complex tissues.

In a recent systematic review by **Urban et al.** [3], assessing the effectiveness of vertical ridge augmentation interventions, It was concluded that although vertical ridge augmentation is a feasible treatment for managing alveolar ridge deficiencies, complications are common. Hence, highlighting the need for exploring novel approaches that would increase the predictability and overcome the current challenges.

3D printing is currently playing an essential role in implant dentistry to design and produce surgical guides and digital models for planning surgical and prosthodontic procedures. However, 3D printed implants or scaffolds for bone reconstruction have not yet been widely adopted in clinical practice.

The following inherent complications and challenges of current bone augmentation procedures in maxillofacial and oral surgeries have increased interest in the utilization of 3D printing technology : morbidity of the autologous graft donor site; technical challenges of the procedure depending on the operator's skill ; the need to prepare both the recipient bed and the collected graft to ensure the fit; and the length as well as invasiveness of the surgical procedures.

3D printing can provide a more precise customized block that conforms precisely to the size and shape of complex defects as well as enabling the customization of the microarchitecture and design of the construct.

One of the unmet challenges inherent in using porous scaffolds, including 3D printed blocks, for the reconstruction of bone in relatively large volume defects is the lack of a suitable matrix that ensures sufficient attraction and accommodation of the migration of host osteoprogenitor and endothelial cells into the interior structure of the implanted scaffold.

During normal physiologic wound healing, It's the blood clot that initially forms in a surgical defect in bone that provides: 1) the fibrin matrix to which host cells can adhere and on which they can migrate; and 2) the platelet-derived growth factors that attract such cells into the defect and stimulated their proliferation and differentiation. These two critically important roles of the blood clot in defects implanted with 3D printed scaffolds are limited by: 1) insufficient bleeding into the interior of the scaffold to form a robust clot; and 2) pre-mature fibrinolysis of the clot will occur before the host cells have been able to migrate into the interior of the block.

Therefore, in this study we hypothesize that osteoprogenitor and endothelial cells will not merely be able to migrate on the walls of the calcium phosphate scaffold; in order for sufficient numbers of these host cells to infiltrate the pores of the scaffold, they require a medium to fill the pores, which mimics the fibrin clot.

With this motivation of finding a substitute for the fibrin clot that can predictably fill the pores of 3D printed blocks for large defects more predictably to overcome the two limitations ,**The global aim of this study was to** develop a gelatin-based gel incorporating platelet-rich plasma lysate, which can be infused into the pores of a 3D printed calcium phosphate block and mimic the role of the blood clot attracting and

accommodating the migration of host osteoprogenitor and endothelial cells into the scaffold and thereby facilitating bone reconstruction and regeneration.

The hypothesis of this research was also that the addition of the PRP lysate into the hydrogel will improve progenitor cells migration into the scaffold and hence improves bone regeneration. Additionally, the hydrogel can act as a delivery vehicle for regulators and growth factors.

Research Background and significance:

Computer-aided 3D printed tissue constructs, have recently opened promising new avenues in tissue regeneration research. It has the unique advantage of offering good control over not only the external shape and form of the tissue but also the micro-architecture of the scaffold. This facilitates the fabrication of customized 3D constructs that conform to complex shapes of bone defects. Furthermore, the constructs performance can be enhanced by several techniques such as cell seeding, incorporation of growth factors and/or drug delivery systems. Jung et al. [4] demonstrated the precision of 3D printed implants and tissue constructs conforming to the unique shapes and forms of different craniofacial defects. This is considered an advantage, in regenerative medicine, that no other technique of manufacturing offers.

Integration of these recent technologies in different fields such as biomaterials science, tissue engineering, regenerative medicine, and cell biology have made 3D tissue regeneration and transplantation possible. Furthermore, it expanded the potential of the use of 3D printed tissue constructs in dentistry and craniofacial defects management [5]. Developing optimized 3D printed scaffolds for bone regeneration will offer less invasive surgical interventions, while promoting tissue regeneration and accelerating the repair process[6]. Consequently, dental implant treatment in patients with insufficient bone width and height can be dramatically improved with fewer complications and more predictable outcomes. Yet, as mentioned before one of the unsolved problems related to the use of porous calcium phosphate blocks for these applications is the absence of a suitable scaffold/matrix within the pores to enable host osteogenic and vascular cells to migrate far enough into the block, proliferate, and thereby synthesize new bone. We believe that advances and novel therapeutics might provide clinicians with biomaterials that offer a more predictable and improved bone regeneration outcomes.

Bone Development, repair, and regeneration:

Although there are some differences between the early embryologic development of bone and its post-natal regeneration and repair conditions. It's worth noting that regeneration can be considered as a recapitulation of bone development. [7]

Wound healing in the oral cavity is one of the biggest challenges for repair and regeneration. The presence of oral fluids containing millions of microorganisms adds up to other local factors that might interfere with the process of healing and consequently impact the potential of repair and regeneration.[8]

The process of bone healing involves the evolution of a series of cellular events that have to occur in a coordinated manner to ensure a predictable repair and regeneration of a bony defect. Many studies in the literature have focused on the hard and soft tissue alterations after tooth loss. Post extraction alveolar process remodeling results in inevitable bone loss that often complicates dental implant therapy.

Alveolar bone remodeling after teeth loss results in loss of dimensional ridge width and height which sometimes can reach 50% of the original anatomy.

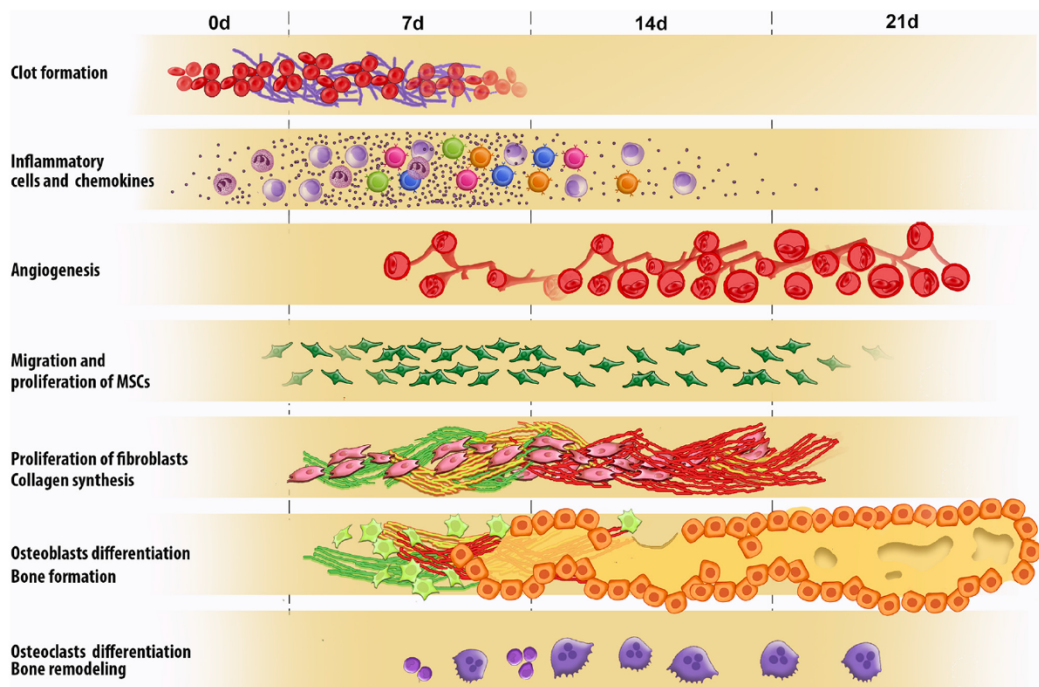
In maxillo-facial surgeries, large alveolar bony defects associated with long-term edentulous patients require complicated, unpredictable and technique sensitive surgeries.

Tremendous efforts have been undertaken by researchers and clinicians to reduce the effects of this inevitable post-extraction hard and soft tissue loss. Yet the available treatment options fail to prevent or fully regenerate the lost tissue in many instances.[9]

Bone healing is a complex process in which the outcome is after dependent on the size of the initial defect. For instance, bony fractures associated with 1mm gap can heal by primary intention as long as blood supply to the area is not compromised.[8]

Understanding the biological events that lead to healing and repair is the key to help coming up with a comprehensive treatment that would lead to a more predictable result limiting inevitable tissue loss and to maximize repair and regeneration outcome.

The initial bone injury is what triggers the bone healing cascade. Bone healing involves the cooperative interplay between osteoblasts and osteoclasts. They work interchangeably and cooperatively to remove defected tissue and regenerate the lost tissue. The first step of this cascade is led by a platelet-driven clot formation. Then the inflammatory process in which growth factors starts to be secreted follows. Some of these factors act as chemokines recruiting endogenous progenitor cells into the defect area to start the processes of cell proliferation, differentiation, and matrix synthesis.[10]



[10]

Figure.1. Schematic figure representing inflammatory and repair events in the bone healing process after tooth extraction. Figure Courtesy: Vieira, A.E., et al.,2015.

Alveolar ridge healing and clinical relevance

Alveolar ridge modeling and remodeling after tooth loss often results in an inevitable bone loss that current grafting surgical interventions and biomaterials sometimes fall short in preventing or restoring large defects. Often times in large defects and severely resorbed ridges, attempting to regenerate this large volume of lost bone tissue requires repeated surgical interventions that might lead to less desirable outcomes. This adequate bone volume is essential to provide a long-term bone support for dental implants carrying acceptable implant-supported prostheses. After tooth loss, the bundle bone that is lining the alveolar socket resorbs, thereafter the modeling and remodeling sequelae leads to altered ridge morphology which reduces vertical and horizontal ridge dimensions. [9, 11] understanding alveolar socket healing is pivotal to set a solid foundation for novel innovations in the field of bone tissue engineering and regeneration.

In a study by **Araujo and Lindhe**, two main phases of alveolar socket healing were described. The first phase involves the bundle bone resorption in which most of the vertical bone loss occurs. A remodeling phase follows afterward marking the second phase during which further reduction in horizontal and vertical bone width and height continues [9, 12]. These Dimensional alterations can jeopardize implant placement in an adequate 3D bone volume and hence its long-term success. It can have a negative impact on the esthetics outcomes, especially in the anterior maxilla where alveolar bone resorption has a more detrimental effect.[11]

Current Grafting techniques, materials, their challenges and shortcomings

Different bone augmentation techniques and materials have been introduced and used along the years to augment and reconstruct alveolar ridge deficiencies. Autogenous bone grafts, alloplasts, xenografts have been utilized in an attempt to maximize the clinical outcomes for these applications. **McAllister and Haghghat** reviewed different guided bone regeneration techniques (GBR) such as the use of Autogenous or allogeneic bone blocks, particulate bone grafts, and distraction osteogenesis. It was concluded that despite

the different procedures available for clinicians to apply, there is a wide range of variability in the outcomes. Each approach is highly dependent on the size of the defect and the case specifics.[13] This highlights the further need for the development of novel biomaterials and approaches that would result in an improved bone regeneration outcome higher predictability.

In a series of studies by **Simion et al.** evaluated the impact of combining recombinant PDGF-BB with a block of deproteinized cancellous bone block in an animal model. The authors highlighted the potential of a significant amount of bone formation in severely resorbed mandibles using only the bone block in combination with PDGF-BB without using a barrier membrane. However, bone formation was not consistent throughout the defect areas. Other challenges mentioned in these studies were fragility of the xenograft that was used in addition to the difficulty in precision encountered during graft trimming. [14, 15]

With 3D printed Blocks, the issue of adaptability and precision can be solved by custom designing blocks according to the complex shape of the individual defects. Using cone beam computed tomography and digital scanning, customized block can be produced to precisely fit the shape of the defect.

In a case report by **Rasperini et al.** using a 3D-printed scaffold for periodontal repair, Limited bone regeneration was noticed histologically. Authors suggested the need to modify the pore interconnectivity and the internal architecture of the 3d printed construct with more surface area.[16]

Currently, autologous bone grafts have been the main source of grafts providing osteoinduction. However, the lack of predictability and the high complications rates reported in the literature has led to a pressing need of investigating novel approaches.

Tissue Engineering Triad, novel approaches and promises for the field: “Tools to optimize regeneration”

Novel Tissue engineering approaches can revolutionize bone reconstruction and regeneration. Currently, research is focused on improving treatment approaches that lead to a predictable, successful yet less invasive bone reconstruction and regeneration

techniques.

Many studies recommended further research using different tissue engineering tools for enhanced bone repair and regeneration.

Pilipchuk SP et al. evaluated recent approaches using regenerative technologies such as scaffolding matrices, cell/gene therapy, and drug delivery to improve bone reconstruction at dental-implant-associated bone defects sites. They concluded that the development of a more optimum scaffold is still needed. It was highlighted that next-generation patient-specific treatments are needed [6].

A recent systematic review evaluated the emerging tissue engineering approaches using tissue Engineering and Regenerative Medicine (TERM) principles [17]. It was emphasized that although the application of these principles demonstrated some clinical success, further studies are needed to achieve meaningful outcomes and approaches.

Therefore, in our study, we revisited the tissue engineering triad, in attempt, to maximize material and design properties for a synergistic effect that would enhance host regenerative potential. (Fig.2)

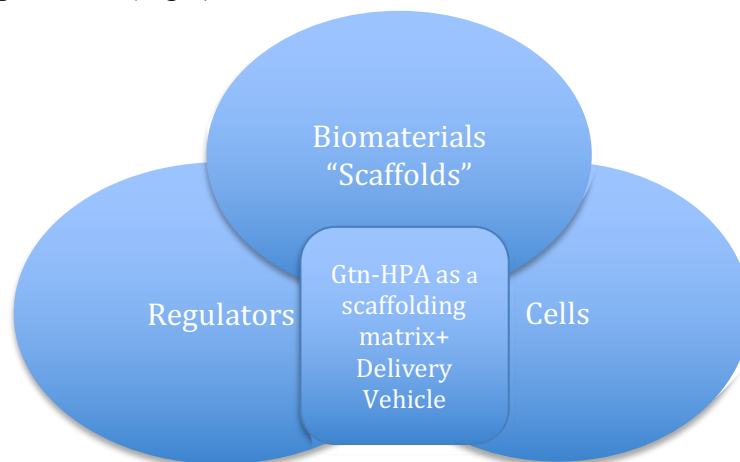


Figure.2. Diagram showing tissue engineering triad, Gelatin-HPA scaffold in our study representing combinatorial treatment modality allowing the interplay of different Tissue Engineering tools.

Platelets and their role in healing

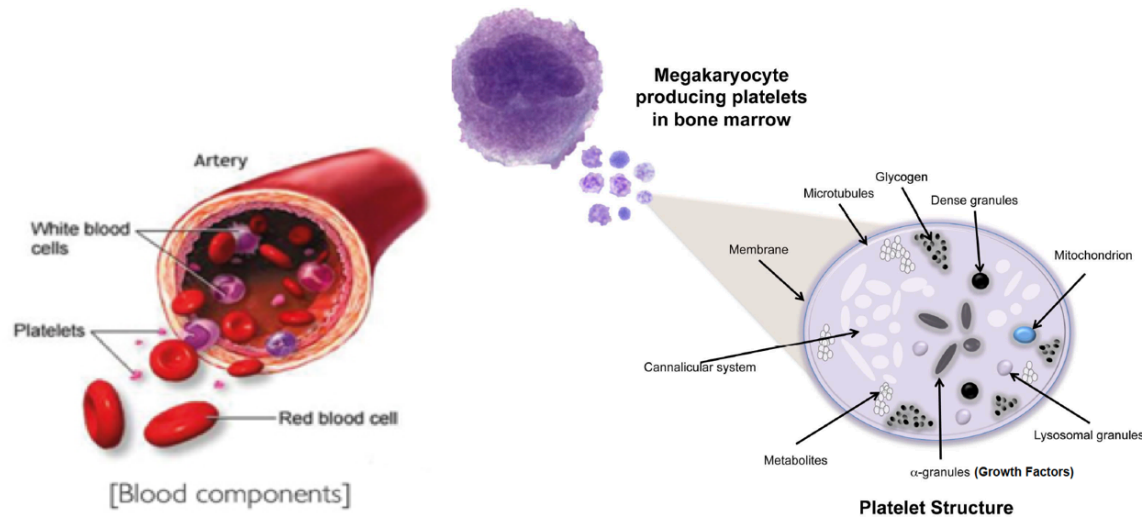


Figure.3. Diagram showing platelets originating from blood vessel injury and their mother cell in the bone marrow

Platelets are non-nucleated blood cells, produced by megakaryocytes in the bone marrow. These cells play a pivotal role in wound healing. They are the driving force behind the initial innate physiologic scaffold in the body which is responsible for hemostasis at the site of the injury. This scaffold (fibrin clot) is then polymerized by thrombin that is released from the platelets.

Moreover, they are a rich source of autologous growth factors. Blood concentrates preparations such as platelet-rich plasma (PRP) contains various growth factors such as platelet-derived growth factor (PDGF), Epidermal growth factor (EGF), Fibroblast growth factor (FGF), Transforming Growth factor β_1 (TGF β_1) and Vascular endothelial growth factor(VEGF).[18]

Growth factors and tissue repair

Mimicking the in vivo complex environment is challenging. Scaffold material, scaffold design, and growth factors should work together to reach the optimal conditions that will serve to replace the originally lost tissue.

However, having the biomaterial or 3D printed constructs alone to repair a defect site is necessary but not sufficient to repair the defect.

In order to enhance the host regenerative ability to repair severe bone defects, the construct needs to be supplemented and paired with growth factors that enhance host regenerative ability to repair and regenerate the defect.

Demonstrating the impact of using growth factors in combination with different scaffold materials; a study carried out by **Lee et al. 2014** [19]. It was concluded that the use of macro-porous CPC with growth factors led to a 2-3 fold increase in new bone formation. The authors suggested that it may be useful to promote bone regeneration in dental, craniofacial and orthopedic applications; and that the mechanical integrity can be improved by the incorporation of a growth factor delivery vehicle.

Our hypothesis is that the migration and differentiation of host cells into the scaffold and the 3D printed blocks will be enhanced by the use of different growth factors to be tested.

Among these therapeutic agents that are currently used biomaterials for bone regeneration applications, such as PRP and PDGF-BB. Although PRP is being widely used nowadays in many bone augmentation procedures, the impact of its benefits is still controversial.

A recent systematic review on the effectiveness of PRP as an adjunct to bone grafting concluded that there is a need for more homogeneous studies to reach a definitive conclusion on PRP impact. [20].

PRP is a good cost effective autologous source of growth factors that are related to improved bone regeneration and angiogenesis and it is readily obtained from whole blood by centrifugation [18]. Since PRP is natural, safe and cost-effective, in our study we investigated the impact of PRP on bone regeneration. Our hypothesis was that PRP will be as effective, if not more, improved migration and bone regeneration compared to PDGF-BB, which has shown improved bone regeneration in many studies of alveolar bone augmentation.

PRP has 7 fundamental growth factors that are secreted by platelets in response to any soft tissue or bone injury. Among these growth factors are the PDGF α and β and the VEGF. PRP also contains 3 proteins in the blood known to act as cell adhesion molecules for osteoconduction and as a matrix for bone, connective tissue, and epithelial migration. The effectiveness and safety of PRP have been proven for many applications in oral maxillofacial and dental procedures [18].

PDGF is a natural signaling molecule produced by the body at sites of bone or soft-tissue injuries that provide two desirable features when it comes to grafting procedures. The first feature is that it induces osteoblasts migration and mitosis at the site of injury promoting bone formation. The second feature is its angiogenic potential promoting neoangiogenesis that leads to the maintenance of graft viability [14].

Nowadays PDGF is being used as an adjunct for treating alveolar ridge deficiencies and periodontal defects. It's produced recombinantly in combination with tri-calcium phosphate. Many studies have shown the beneficial effect of PDGF-BB on bone regeneration when added to different grafting materials. **Simion et al 2007[15]** showed that the combination of PDGF with a deproteinized bovine block, without the placement of a barrier membrane, had the potential to regenerate significant amounts of new bone in severe mandibular ridge defects.

Additionally, **Cerruti et al. 2007** [21] performed a study to combining platelet-rich plasma (PRP) and mononuclear cells from bone marrow (MSC) aspirate with a bone scaffold for bone augmentation in the maxillae. They concluded that MSC and PRP promote adequate integration of the graft.

In another study performed by **Marx et al. 2013** [22] evaluating the effect of using a composite graft of recombinant human bone morphogenic protein-2/acellular collagen sponge (rhBMP-2/ACS) , crushed cancellous freeze-dried allogenic bone (CCFDAB) ,and platelet-rich plasma (PRP) compared to 100% autogenous bone in large vertical defects of the maxilla. It was concluded that using the composite graft greatly reduced the morbidity inherent in autologous bone harvesting. Additionally, it regenerated a functionally stable bone, equal to an autologous bone graft, with greater vascularity and less residual bone particles.

The therapeutic use of growth factors to improve bone regeneration still has limitations such as their costly purification process, quality reproducibility, their short half-life and establishment and maintenance of the effective dosage in physiological conditions, that varies according to the different clinical applications.

Knowing these limitations and attempting to overcome the limitation of the short half-life of growth factors, is an important challenge to overcome in novel therapeutics. In this study, we are proposing the application of a gelatin hydrogel that will first act as a reservoir for the growth factors extending their release for longer time periods. Secondly, the gel will act as a space maintaining device and a matrix scaffold enhancing the required host cells migration, differentiation, and proliferation into the 3D printed scaffold to fill the bony defect.

Based on the literature discussed above, we believe that host regenerative ability can be improved and fueled by using bioactive agents incorporated to help to modulate the process of healing.

Hydrogels and their current applications in regenerative medicine therapeutics

Advances in the field of bioengineering, biochemistry, and nanotechnology led to the development of Hydrogels that had unparalleled novel properties that can be customized precisely for specific desired delivery applications.[23, 24]

Among the different types of hydrogels available, stimulus-responsive hydrogels have the peculiar capability of drug delivery and in situ gel formation. In situ gellable hydrogels has been used in many applications in the medical and pharmaceutical fields for drug delivery. Enzymatically cross-linked gelatin gels have the unique advantage of tunable proteolytic degradability by controlling the amount of peroxidase concentration.

Moreover, since these hydrogels can be injected in a liquid form, which undergoes covalent cross-linking, so they conform to any shape allowing homogenous incorporation of therapeutic molecules or cells. [25],[26].

In this project, an in situ gellable hydrogel - formed by the Horseradish peroxidase (HRP-mediated crosslinking reaction) - will be used to carry the different growth factors used. The injectable Gelatin-Hydroxyphenylpropionic acid (Gtn-HPA) gel has shown success in proliferation, migration, and differentiation of neural stem cells and human mesenchymal stem cells. Moreover, in an in vitro study by **Lim et al.** evaluating differentiation and migration of adult neural stem cells (aNSCs), it was found that the viability of the cells was higher in the Gtn-HPA scaffolds, when compared to the collagen ones even at high concentrations of H₂O₂ reaching 500μM. This suggests that the mechanism by which Gtn-HPA undergoes crosslinking helped in increasing the cells resistance to oxidative stress by preconditioning the cells to sub-critical levels of oxidative stress [27], [28].

In this study, we hypothesize that Gtn-HPA can serve both as a scaffolding matrix allowing cell migration of host cells into the bony defect in addition to acting as a delivery vehicle for the sustained release of therapeutic agents over extended periods of time.

The duration of the drug release from hydrogels delivery systems available nowadays is usually limited a maximum of few days. For clinical applications, this period has to be extended, especially if the hydrogel will be implanted.[24]

Another advantage of using the Gtn-HPA is that the rate of degradation and cross-linking are controllable through the concentration of horseradish peroxidase(HRP) and hydrogen peroxide (H₂O₂) which is a critical property for tissue engineering applications [29]

In a study by **Wang et al.**, promising results were obtained for osteochondral repair in a rabbit model. The role of hydrogel stiffness had had a significant impact on the improved cartilage formation along with smoother integration.[30] Moreover, Gtn HPA is being studied nowadays in many other regenerative medicine applications such as spinal cord injuries and brain lesions. Few studies focused on the use of these gelatin-based hydrogels and bone regeneration. one study by **Chun et al.** [31] developed a hydrogel-bioceramic composite, which demonstrated improvement in cell functions that promote bone regeneration.

A current study being done in our laboratories has Preliminary promising results using the hydrogel in brain lesions, of a rat model, have shown the longest-term in vivo evaluation of a rat stroke model. After 10 weeks post injection of Gtn-HPA gel carrying EGF as a growth factor, the hydrogel was still present in areas into which cells have not yet migrated.

Significance:

1. Overcoming the unmet challenge of the use of porous calcium phosphate blocks for reconstruction of large alveolar bone deficiencies which is the absence of a suitable scaffold/matrix within the pores to enable host osteogenic and vascular cells to migrate into the interior of the block, proliferate, and synthesize new bone.
2. Supporting the short-lived fibrin clot and providing a more robust and stable alternative to act as a scaffold that can remain for substantial periods of time necessary allowing the host resident cells to migrate into the center of the large defect and to synthesize their matrix.
3. Improving host regenerative ability using PRP-Lysate as a source of different growth factors that might lead to shortening of treatment time.
4. Future Clinical Applications: targeting patients with large vertical and /or horizontal bone deficiencies and paving the way to create an effectively customized bone scaffold for bone regeneration, thereby offering a less invasive bone block augmentation technique.

Innovation:

1. The PRP Lysate-infused hydrogel as a chemoattractant for cell migration and differentiation.
2. The novel clinical future targeted application we are proposing is infusing the 3D printed porous blocks with the Gtn-HPA incorporating PRP-lysate into the pores of the porous blocks for improved bone regeneration.
3. Using the Gtn-HPA with its peculiar tunable cross-linking density and characteristic nano-fibrillar structure into the porous blocks would be one of the novel solutions for finding the optimal pore size, interconnectivity and internal architecture of 3D printed blocks. “In situ tunable pore size adjustment”.
4. The developed hydrogel will not only act as a scaffold for bone reconstruction but also act as a delivery vehicle for the sustained release of different growth factors allowing their release from the hydrogel.

Hypotheses and Specific aims:

The **global objective** of this research was to develop a gelatin-based gel incorporating platelet-rich plasma lysate, to mimic the role that a blood clot would normally play to attract and accommodate the migration of host osteoprogenitor and endothelial cells into the scaffold to facilitate bone reconstruction. With the hypothesis that the addition of the PRP lysate into the Gtn-HPA hydrogel will improve progenitor cells migration into the scaffold and hence improves bone regeneration.

Specific aim#1: Cell Migration into the hydrogel *In Vitro* “cell migration assay”

To investigate the migration of rat marrow-derived mesenchymal stem cells (MSCs) into gelatin-hydroxyphenyl propionic acid (Gtn-HPA) hydrogel under the influence of **rat-platelet rich plasma (PRP) lysate incorporated into the gel.**

Hypotheses:

- Gtn-HPA hydrogel enables MSC migration.
- PRP-lysate increases MSC migration into the hydrogel.
- PRP-lysate demonstrates comparable or better results compared to recombinant PDGF-BB.

Specific aim#2: Assessing cell differentiation and osteogenesis in PRP-Lysate infused

To assess the permissibility of the Gtn-HPA hydrogel of differentiation of MSCs into osteogenic cells and the influence of using PRP-Lysate.

Hypothesis:

We hypothesize that the incorporation of PRP lysate into the hydrogel scaffold improves bone regeneration.

Specific aim#3: Gtn-HPA acts as a Delivery Vehicle for growth factors

To evaluate the growth factor release profile of PDGF-BB and EGF from the Gtn-HPA infused with 2 different PRP-Lysate preparations and pure recombinant rat- PDGF-BB.

Hypothesis:

Gtn-HPA will not only serve as a scaffold but also can act as a delivery vehicle that allows sustained and controlled release of the infused therapeutic agents over extended periods of time.

Aims Outcome measures samples grouping and Study Design:

- **Specific Aim#1 Outcome measure:**
migration of rat marrow-derived mesenchymal stem cells (MSCs) into gelatin-hydroxyphenyl propionic acid(Gtn-HPA) hydrogel in vitro assessed by cell count analysis based on DAPI stained nuclei using confocal microscopy and quantification using **Image J** software.

I. Cell migration assays:[32]

In this study, a core-ring 3D in vitro model was used Cell migration assay was carried out using Rat bone marrow MSCs.

samples grouping was as follows:

Group 1: “control group” in which the blank Gtn-HPA hydrogel was used

Group 2: PRP lysate infused Gtn-HPA hydrogel

Group 3: Pure recombinant PDGF-BB infused Gtn-HPA hydrogel

Specific aim#2 Outcome measure:

To differentiation was performed using confocal microscopy by immunostaining for Anti-osteocalcin antibody, then measuring area% of osteocalcin + cells using ImageJ software for comparison among the experimental groups.

- **Group 1 “Control”:**
Blank rat-MSCs seeded Hydrogel + Cell expansion medium “CEM”
- **Group 2 “+ve control group”:**
Blank rat-MSCs seeded Hydrogel + Osteogenic medium “OM”
- **Group 3:**
rat PRP -lysate infused cell-seeded hydrogel + “OM”
- **Group 4:**
PDGF-BB infused cell-seeded hydrogel + “OM”

Specific Aim #3 Outcome measure:

To investigate PDGF and EGF release profile from the 2%Gelatin-HPA hydrogel using an enzyme-linked immunosorbent assay ELISA.

Sample Grouping:

with N=5 the experimental groups were divided as follows:

A. For the PDGF release assay:

Group 1: the blank hydrogel

Group 2: Hydrogel + PRP lysate I

Group 3: Hydrogel + PRP lysate II

Group 4: Hydrogel + 50 ng PDGF –BB

B. For the EGF release assay:

Group 1: the blank hydrogel

Group 2: Hydrogel + PRP lysate I

Group 3: Hydrogel + PRP lysate II

Sample size determination:

we propose 6 animals per group to be used for power calculation. Aiming to determine a significance of 30% difference in a selected outcome variable such as the amount of bone filling the defect comparing the 3D printed block alone as the control group to the block with the hydrogel. A 15% standard deviation for both groups $\alpha=0.05$, and $\beta=0.05$.

Our hypothesis is that the difference between the groups (groups of defects with and without the 3D printed block of more than a 30% for a particular outcome would be necessary for the 3D block to likely be of clinical importance.

Materials and methods:

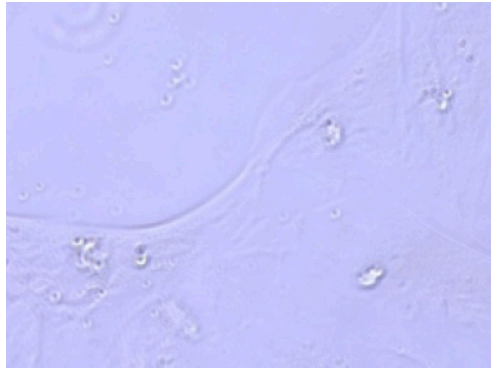


1. Cells "Rat MSCs Cell Lineage differentiation assay":

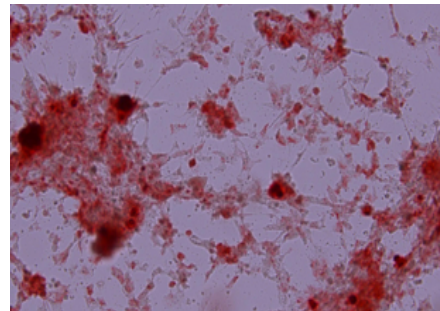
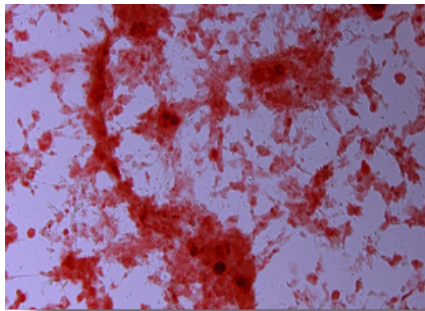
Rat MSCs used in this study were isolated in our lab from tibia and femurs of SD adult rats >3months old following protocol[33], used cells were passaged and grown until used at passage 3 or 4 P3/P4 for all experiments. Adipogenesis and Osteogenesis Cell lineage differentiation was performed beforehand. Cultured cells at passage 3 were seeded in a six-well cell culture plate. When the cells reached 80% confluence, they were still cultured in DMEM-LG supplemented with 10% FBS (as a control) or treated in osteogenic differentiation medium or adipogenic differentiation medium, respectively. For the osteogenic differentiation medium: DMEM-LG supplemented with 10% FBS, 0.05mM ascorbic acid, 10mM β -glycerol phosphate and 100nM dexamethasone. Adipogenic differentiation medium: DMEM-HG supplemented with 10% FBS, 1 μ mol/L dexamethasone, 10 μ g/mL insulin, 500 μ M 1-methyl-3-isobutylxathine (IBMX) and 1 μ mol indomethacin. The medium was changed every other day for 21 days. After 21 days, cells were then fixed using 4% paraformaldehyde left overnight. Histochemical staining was then performed to assess differentiation based on morphology.

Images were taken using Olympus inverted light microscopy using objective lens 10x.

a)



b)



c)

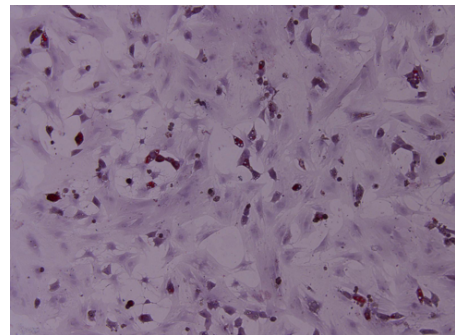
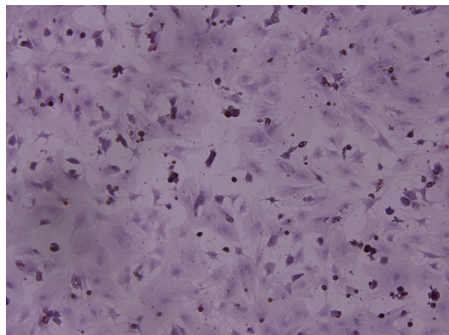


Figure.4. Cultured Rat-MSCs cells were able to undergo osteogenic and adipogenic differentiation in a 21 days lineage differentiation assay (A) undifferentiated cultured rat-MSCs (B) Alizarin Red S staining showing the calcific nodules formed after 21 days indicating osteogenic differentiation of the cells. (C) Oil Red Staining for adipocytes and the formed fat globules in red and the dramatic change of cell morphology shown with Hematoxylin and Eosin (H&E) staining.

The cultured cells at passage 2 were seeded in the plastic culture flasks at 5×10^5 /bottle. Cells were passaged and used when they grew at 70% confluence, continuously cultured in cell expansion medium DMEM-LG supplemented with 10% FBS, 100 U/mL streptomycin, 10 ng/mL FGF-2, 100 U/mL penicillin. Each 75cm^3 cell culture flask was supplemented with a 25 mL medium and changed every 2d.

2. PRP-Lysate extraction and preparation protocol:

whole rat blood (8ml) was collected into sterile syringes containing 2ml of anticoagulant citrate dextrose solution (ACD), with ACD to whole blood ratio of 1:4. The whole blood was initially centrifuged at 1200CRF for 2 minutes. PPP and PRP layers were collected in a separate tube called plasma 1 as shown in **Diagram [1]**. a second centrifuge for the remaining blood at 1200 CRF was done, PPP and PRP layer was collected and that was plasma 2. Plasma 1 and plasma 2 were then added together in another tube for the 3rd centrifuge at 1200 CRF for 5 minutes. Platelets activation was done using 250ul of 10%CaCl₂ added into 10ml of PRP for activation according to platelet activation protocol by **Textor et al.**[34]

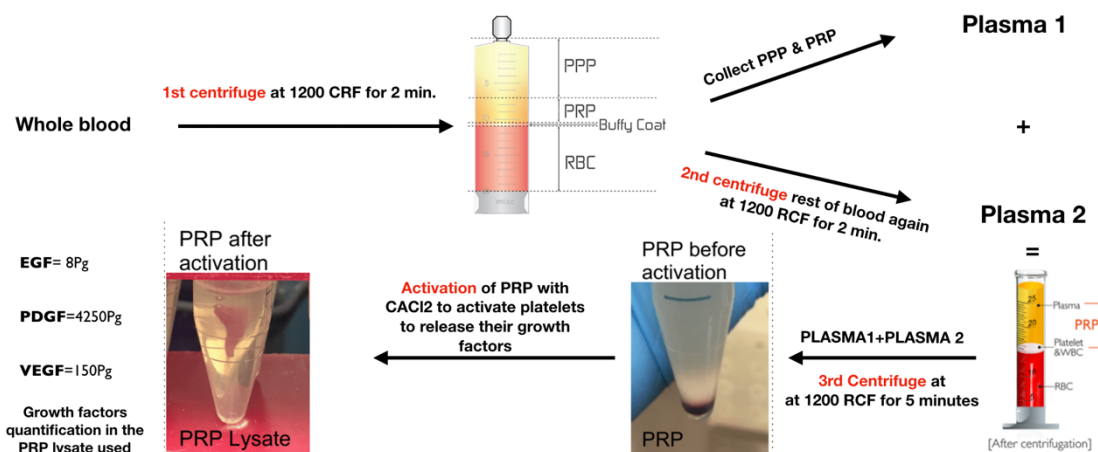


Figure.5. Diagram showing the processing method performed in our lab to obtain PRP-Lysate. ELISA quantified growth factors in the PRP-Lysate used in the migration assay is shown on the left.

PRP Standardization and growth factors quantification

PRP from blood extracted from SD rats >3 months old was extracted and prepared using a standardized repeatable protocol developed by our lab (see Fig.5).

An aliquot of the PRP-lysates prepared was taken for ELISA testing to quantify the number of different growth factors present for each experiment done.

PDGF-BB, VEGF, and EGF concentration quantification were done using an enzyme-linked immunosorbent assay (ELISA) kit (Rat-PDGF, EGF and VEGF Kits R&D USA).

3. Rationale and development of Gtn-HPA formulation

Gtn-HPA gel synthesis and fabrication:

Wang et al. developed Gtn-HPA Hydrogels to be used as scaffolds for tissue engineering applications[35]. The gelatin-hydroxyphenyl propionic acid conjugate was obtained from Dr. Motoichi Kurisawa at (A*STAR) Agency of Science, Technology, and Research. Gtn-HPA synthesis occurs on two main steps. The First step is that the Lyophilized gelatin conjugate (Gtn) and 3-(4-hydroxyphenyl) propionic acid (HPA) are prepared from raw materials as seen in (figure 6). The second step is the Gtn-HPA matrix preparation which takes place by covalently cross-linking the Gtn-HPA Conjugate with horseradish peroxidase(HRP) and hydrogen peroxide through the HRP –catalyzed crosslinking mechanism. This reaction is driven by 3 components, the gelatin content, HRP and H₂O₂ concentrations, so different concentrations can be chosen according to the desired properties of the Gtn-HPA hydrogel and according to the application it will be used for.

A. Gtn-HPA conjugates synthesis:

the conjugates were prepared through a general carbodiimide/active ester-mediated coupling reaction in distilled water. A mixture of 250ml distilled water and N, N-dimethylformamide(DMF) (3:2) were used to dissolve HPA(3.32g,20mmol). Another mixture of N-hydroxysuccinimide (3.20g,27.8mmol) and 1-ethyl-3-(3-di-methyl amino-propyl) carbodiimide hydrochloride(3.83g,20mmol) was then added to the first mixture. Stirring for this reaction was performed at room temperature for 5 hours, and the PH of the mixture was maintained at 4.7. Afterward, the solution was dialyzed in dialysis tubes against 10mM sodium chloride solution for 2 days. For day one 25% ethanol in distilled water and for the second day distilled water only was used. Finally, the purified solution was lyophilized to obtain the Gtn-HPA conjugate. “The conjugate was obtained from Dr.Motoichi Kurisawa, A*STAR, Agency of Science, Technology and Research [35]

B. Gtn-HPA Hydrogels Synthesis:

3D Gtn-HPA hydrogels were produced by first preparing a Gtn-HPA conjugate Solution for the intended final gelatin concentration planned for the migration assay experiment (2%).

In this study 4% Gtn-HPA solution was prepared first by dissolving the lyophilized Gtn-HPA conjugate in PBS for a final concentration of 40mg/ml in PBS. The solution was then kept for one hour at 37°C for complete dissolution of the Gtn-HPA conjugate.

The gel formulation used was crosslinked as described below in Table [1]. 0.1U/ml HRP and 1.2Mm H₂O₂ were added to the solution for gelation.

Formulation	Gtn-HPA	HRP	H ₂ O ₂	Gelation Time
4% Gtn-HPA	40 mg/ml	0.1U/ml	1.2mM	~1 minute

Table.1. Gtn-HPA formulation and the concentrations of the constituents

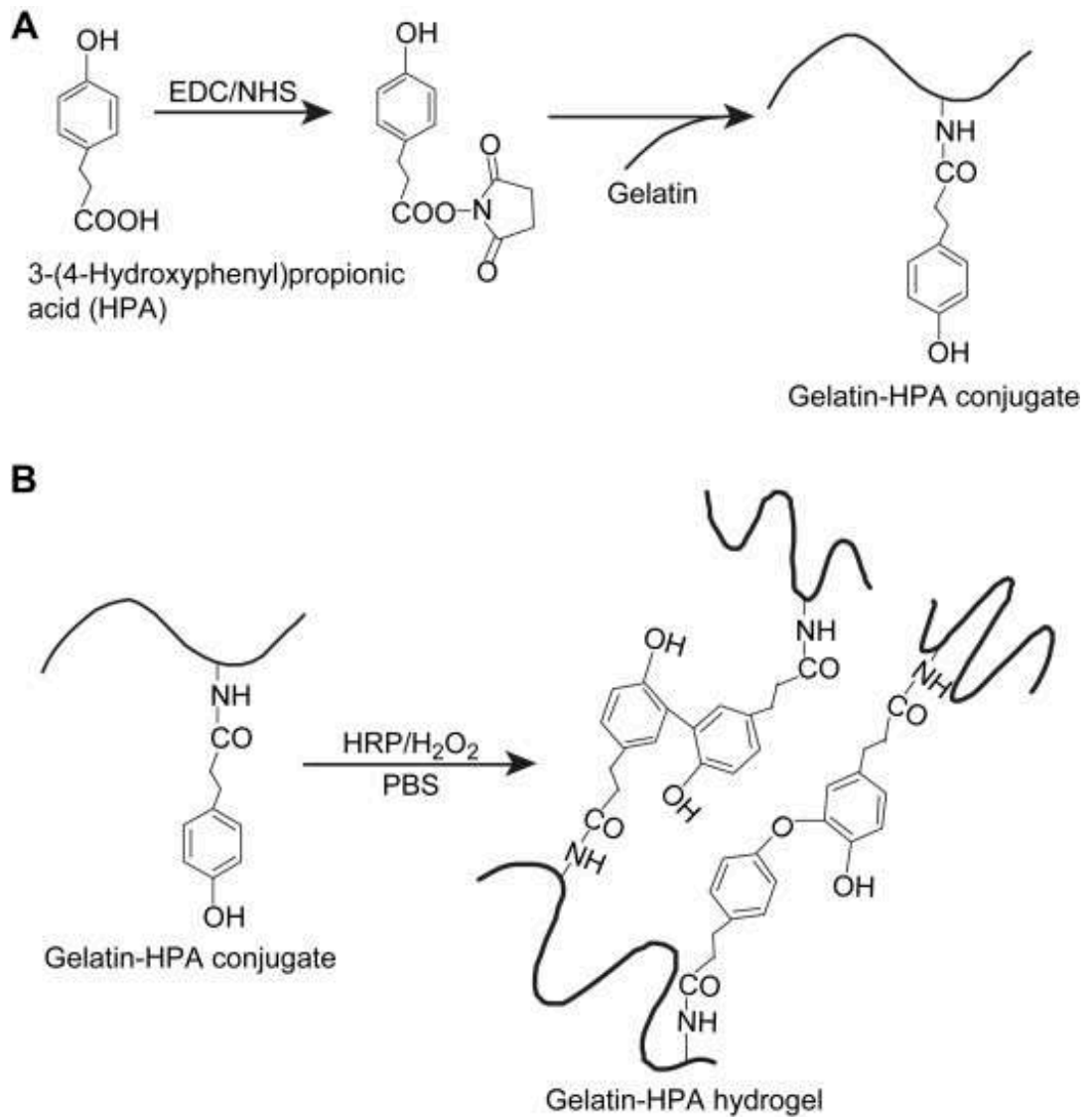


Figure.6. Schematic Drawing for the two-step fabrication of Gtn-HPA gel (A) A non-crosslinked Gtn-HPA conjugate is prepared using gelatin (Gtn) and 3-(4-hydroxyphenyl) propionic acid (HPA). Gtn-HPA conjugate can be lyophilized to be used for later experiments (B) Gtn-HPA gel is prepared by enzymatic HRP-catalyzed crosslinking mechanism using horseradish peroxidase (HRP) and hydrogen peroxide (H₂O₂). Figure courtesy – Hu et al Biomaterials, 2009. 30(21): 3523-3531

I. Core-Ring 3D assembly migration assay:[32]

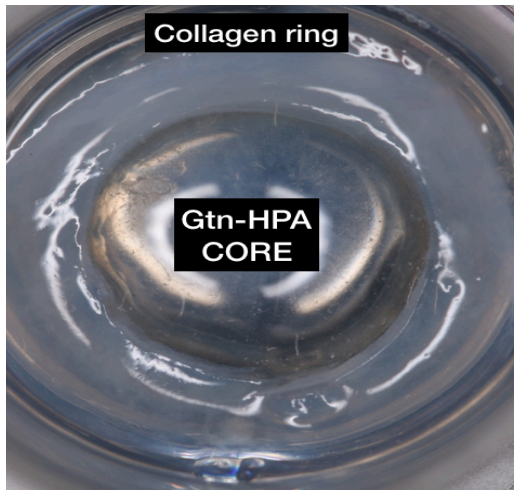


Figure 7. Photo of the migration assay sample showing the Collagen Ring and the core Gtn-HPA hydrogel.

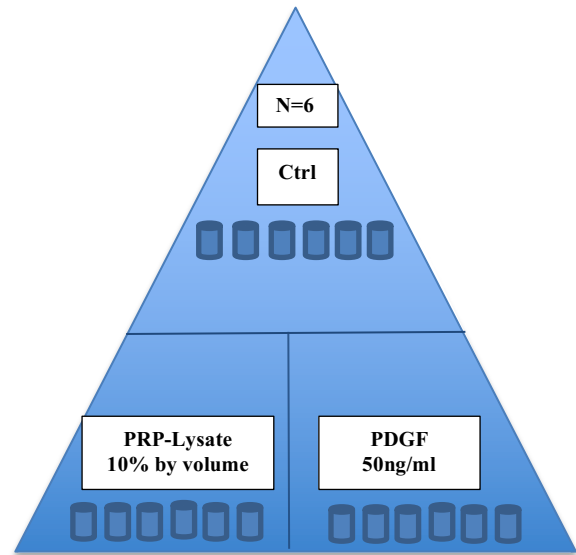


Figure 8. Diagram showing the sample grouping for the migration assay and their respective growth factors concentrations used for the migration assay. Sample showing the Collagen Ring and the core Gtn-HPA

Each sample out of the total six samples for each of the experimental groups as shown in (Fig.8) were casted on the wells of a 24-well cell culture plate. The base of each well was prepared and covered by 1ml of 2% agarose solution, then collagen ring around the core Gtn-HPA hydrogel were casted as described below:

After 4% Gtn-HPA was prepared as described earlier, the final 2% Gtn-HPA used for the experiment was obtained by adding pure Dulbecco's modified eagle medium (DMEM from Life Technologies,USA) with a ratio of 1:1. 10% PRP-Lysate was incorporated into the gels for the PRP-lysate group, as for the PDGF experimental group ,50ng/ml of rat-PDGF-BB was incorporated into the hydrogel. Afterward, 250 μ l of the 2% hydrogel was casted as the core gel and left for gelation at 37°C for 30 minutes. Then rat-MSCs seeded collagen rings were casted around each core gel. 350 μ l of 0.8mg/ml type I collagen solution with the rat-MSCs cell density of 0.2million cells/ml was casted around each core gel then incubated for 2h. at 37°C. Finally, 1ml of DMEM +10%FBS+1% was added, then changed every other day.

Immunostaining:

After 10 days, all samples were fixed using 1ml of 4%Paraformaldehyde at 4°C overnight. Samples were then stained according to manufacturer immunostaining protocol with DAPI, anti α SMA (Sigma Aldrich#A5228) , Anti-CD105 antibody and KI67 staining (Abcam, USA). The time allowed for the primary and secondary antibodies to penetrate into the 3D casted hydrogels was 24 hours.

Samples Immunostaining and quantification of migrated cells using Confocal microscopy and image J software:

After DAPI and other previously mentioned markers immunostaining. DAPI staining was used mainly to quantify the nuclei of migrating rat MSCs confirmed with other markers such as CD105 and α SMA. Confocal laser scanning microscope (Nikon Eclipse C2+ laser scanning system) (Fig.9) was used to image migrating cells in the 3D core gel across the interface between the collagen ring seeded cells and the core Gtn-HPA as shown in (Fig.10).

Images of Four different regions of interest of migrated rat-MSCs across the ring-core interface were selected randomly for each sample. The images were then exported to image J software (U.S. National Institute OF Health, Bethesda, MD, USA) for quantification of migrated cells. DAPI fluorescence was used on image J software to obtain the migrated cells count traversed across the interface. The average cell count of the four selected areas for each well was then used for the statistical analysis.

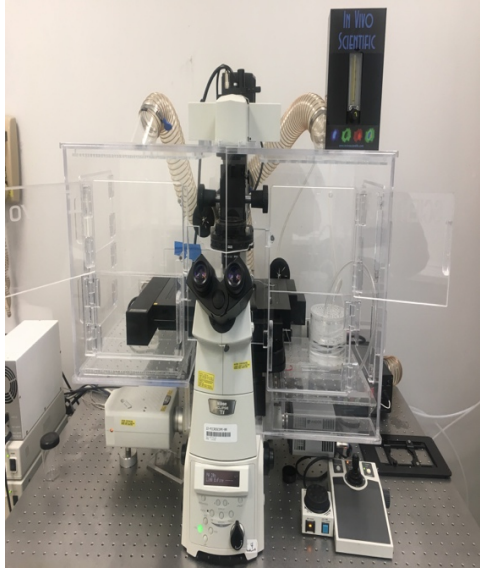


Figure 9. Nikon Eclipse C2+ laser scanning system confocal microscopy used for imaging

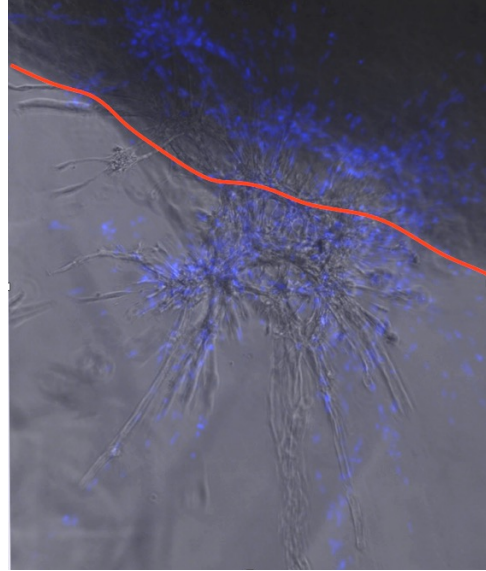


Figure 10. showing superimposed Image of one of the samples showing the DAPI stained nuclei image superimposed on the Bright field image to illustrate the demarcation of the interface between the collagen ring and the core-Gtn-HPA hydrogel depicted by the red line.

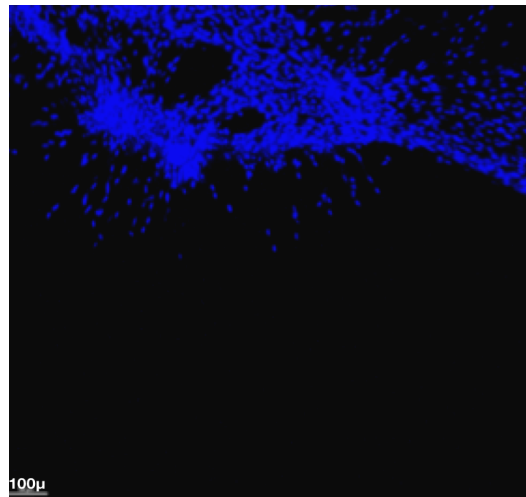
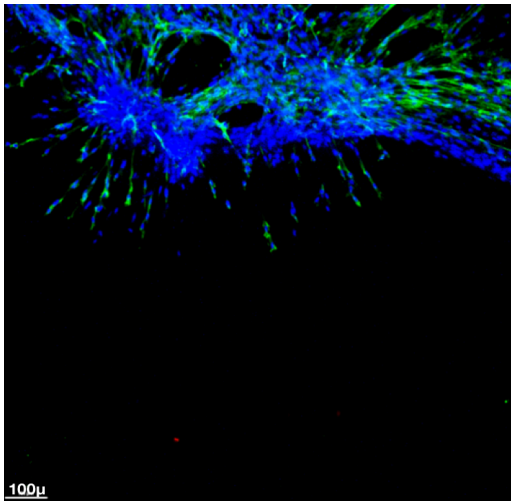


Figure 11. Confocal microscopy images using 10x Macro objective lens. Left photo: showing double staining DAPI/Anti α SMA elucidating the pattern of migration of the rat-MSCs from the collagen ring into the Gtn-HPA core hydrogel. Right Photo: showing an example of a DAPI stained nuclei image that was used for quantification on Image J quantification.

II. Assessing cell differentiation and osteogenesis assay in PRP-Lysate infused cell-seeded hydrogel:

In this experiment, the experimental groups were divided into 4 groups with N=6, as follows according to medium type and growth factors incorporated in the gel:

Group 1 “control group”: in which a blank cell seeded Gtn-HPA hydrogel was used + Cell expansion medium (CEM).

Group 2: “Positive control” Blank rat-MSCs seeded Gtn-HPA hydrogel + Osteogenic medium (OM).

Group 3: PRP lysate infused rat-MSCs seeded Gtn-HPA hydrogel (10% volume) + OM
Group 4: recombinant rat-PDGF-BB infused rat-MSCs seeded Gtn-HPA hydrogel (50ng/ml) + OM.

48-well cell culture plate prepared as mentioned in the previous experiment was used. With a cell density of 0.1 million rat-MSCs cells/ml, 200 μ l of the prepared 2% Gtn-HPA cell-seeded hydrogels were casted on each well for the 6 samples of each experimental group.

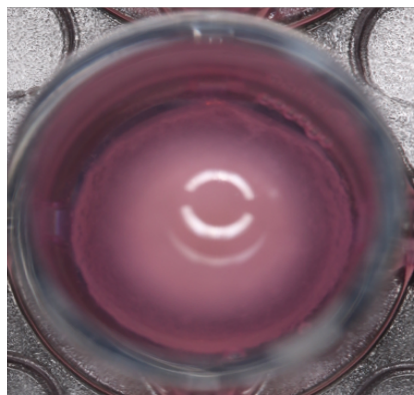


Figure 12. showing a sample of the cell seeded gelatin-HPA hydrogel casted in the well of 48-well cell culture plate.

After 28 days, all samples were fixed using 4% paraformaldehyde overnight. Immunostaining then was done for Anti-Osteocalcin antibody, Anti-SP7/ Osterix antibody and DAPI (Abcam). Each of the primary and secondary antibodies was left for 24 hours to allow penetration through the 3d hydrogel constructs following protocol shown in [Table 2.]

For imaging, confocal microscopy was used using the 10x macro objective lens. Images were then exported to Image J software for quantification. Area percentage covered by the selected osteogenic marker of interest (Anti-Osteocalcin antibody) fluorescent signal expressed by cells in the hydrogel for each sample across the groups was calculated. The calculated percent area data was then used for the statistical analysis and comparison among the groups.

Primary Antibody	Dilution	Secondary antibody
Mouse anti-osteocalcin antibody(abcam#ab13418)	1:80	Green-Alexa 488 anti-mouse
Rabbit anti-SP7 / Osterix antibody(abcam#22552)	1:500	Anti-rabbit Red Cy-3

Table.2. showing Anti-Osteocalcin Antibody and Anti-SP7/Osterix immunostaining protocol used

III. The release profile of PDGF from PRP lysate and pure PDGF-BB Gtn-HPA infused hydrogels:

a) PDGF

Studying the release of PDGF was important to determine whether the Gtn-HPA act as a delivery vehicle that allows sustained and controlled release of the infused therapeutic agents over extended periods of time.

Four experimental groups were studied with N=5 for each group:

- 1) 2% Gtn-HPA blank hydrogel
- 2) PRP Lysate preparation I-infused Gtn HPA.
- 3) PRP Lysate preparation II-infused Gtn-HPA.
- 4) Pure recombinant Rat PDGF-BB infused Gtn-HPA.

For the PRP Lysate preparations' I and II original PDGF concentration were quantified. They were 1561pg/ml and 1604.1pg/ml respectively. Regarding the pure PDGF-BB group the concentration used was 50ng/ml. The concentrations of the 2% gel formulation constituents are shown in table [1].

Gel Formulation	Gtn-HPA	HRP	H₂O₂	PDGF
Blank gel	40mg/ml	0.1u/ml	1.2mM	0
2% Gtn-HPA /PRP lysate preparation I (10% PRP)	40mg/ml	0.1u/ml	1.2mM	1561.84Pg/ml
2% Gtn-HPA/PRP lysate preparation II (10%PRP Volume)	40mg/ml	0.1u/ml	1.2mM	1504.1Pg/ml
2% Gtn-HPA/PDGF-BB	40mg/ml	0.1u/ml	1.2mM	50ng/ml

Table.3. Showing Experimental groups for PDGF release study with the concentration of the Gelatin-HPA fabrication constituents.

After fabrication of the 2%Gtn-HPA, 250µl of the gel casted for each sample in a 2ml cryotube, gels were submerged in 1.5 EBSS release buffer .750µl of the supernatant was collected at the following time points to study the release of PDGF: Day 0 1h, day 2, day4,6,10,14,20,28 followed by addition of 750µl of fresh EBSS each time. 28 days' time test period was chosen to represent an extended time period of growth factor release needed for early bone formation and it was the time point where the osteogenesis assay was fixed as well.

Growth factors concentration in the collected supernatants at the different measured according to the manufacturer's instructions. Rat PDGF-BB ELISA kit (R&D Systems). All assays were performed in duplicates.

b) EGF:

Three experimental groups of N=5 were studied as follows:

- 1) 2% Gtn-HPA blank hydrogel.
- 2) PRP Lysate preparation I infused Gtn-HPA.
- 3) PRP Lysate preparation II infused Gtn-HPA.

For the PRP-Lysate preparations gel was incorporated with 10% volume ratio as described previously in the gel preparation. Supernatants were collected at the same time points as done for PDGF. Rat-EGF ELISA Kit (R&D Systems, USA) was then used. All assays were performed in duplicates.

Gel Formulation	Gtn-HPA	HRP	H₂O₂	EGF
Blank gel	40mg/ml	0.1u/ml	1.2mM	0
2% Gtn-HPA /PRP lysate preparation I (10% PRP)	40mg/ml	0.1u/ml	1.2mM	3.6Pg/ml
2% Gtn-HPA/PRP lysate preparation II (10%PRP Volume)	40mg/ml	0.1u/ml	1.2mM	4Pg/ml

Table.4. Showing Experimental groups for EGF release study with the concentration of the Gelatin-HPA fabrication constituents.

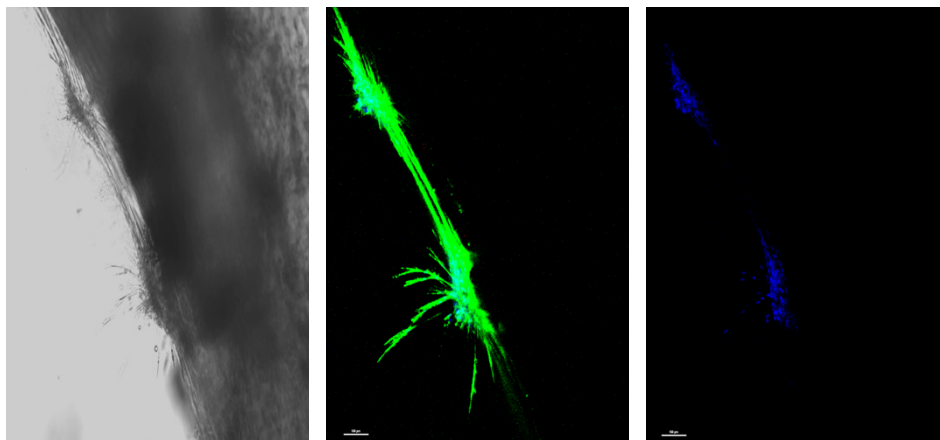
Results:

Gtn-HPA was permissive to cell migration, PRP Lysate displayed increased rat MSC migration into the Gtn-HPA compared to the blank gel and the PDGF-BB containing hydrogel.

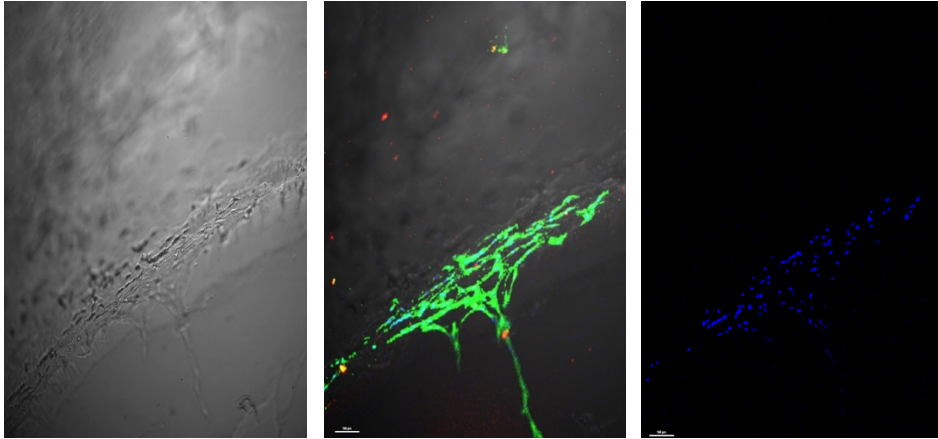
The results of the migration assay showed that the number of MSCs migrating into the hydrogel was significantly higher in the PRP lysate- incorporating hydrogel group (640 ± 240 ; mean \pm SD) compared to the PDGF-BB (196 ± 81) and the blank gel control groups (160 ± 41); $n=6$; p -values were 0.0006 and 0.0003, respectively.

Moreover, a certain migration pattern for all the groups (Fig.13) was evident as depicted by the Anti- α - SMA staining of the cell's cytoskeleton. However, it was more robust for the PRP-lysate group. This cell migration pattern took the form of trees branching out across the ring-core interface in tufts like structures towards the Gtn-HPA core gel. α SMA staining helped to accentuate the migration pattern by staining the cell's cytoskeleton.

A.



B.



C.

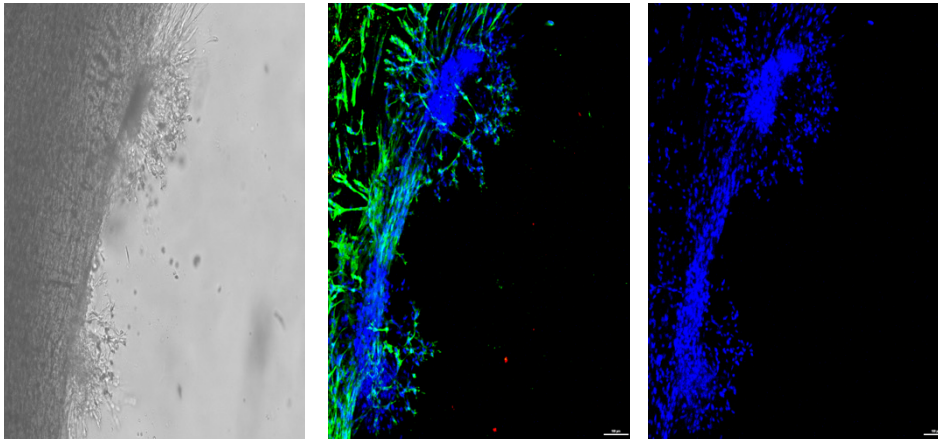


Figure 13. Representative DAPI(Blue)/Anti α -SMA(Green) immunostained hydrogels, showing the Ring/Core interface and the migrating rat-MSCs into the core Gtn-HPA. (A)Control (B) PDGF-BB group (C)PRP-Lysate group:

GROUPS	Sample 1 cell count	Sample 2 cell count	Sample 3 cell count	Sample 4 cell count	Sample 5 cell count	Sample 6 cell count	Mean	SD
Blank Gtn-HPA	155	142	181	121	24	335	159.66	101.42
Gtn-HPA/PDGF-BB	269	157	128	144	325	155	196.33	80.62
Gtn-HPA/PRP	355	1065	522	540	690	666	639.66	240.39

Table.5. Quantification of migrated cells across the collagen ring/Gtn-HPA core interface among the different experimental groups. The cell count was done after 10 days of the migration assay based on DAPI stained nuclei using Image J software.

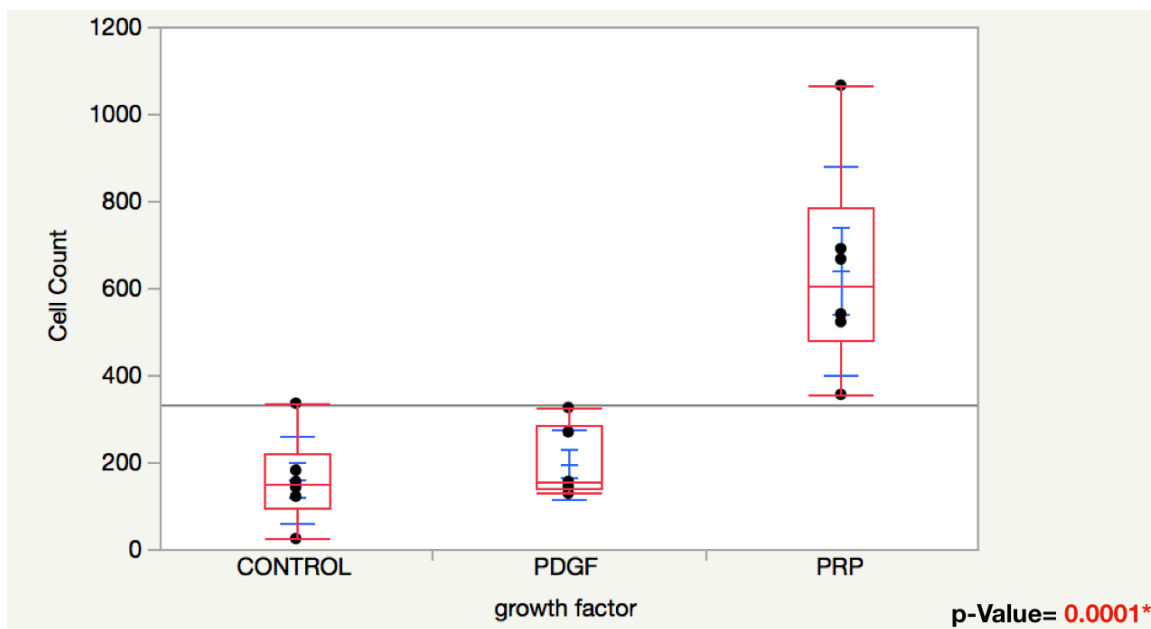


Figure.14. Graph showing one way-ANOVA analysis for the migration assay “Cell Count” by “Growth Factor” among the groups

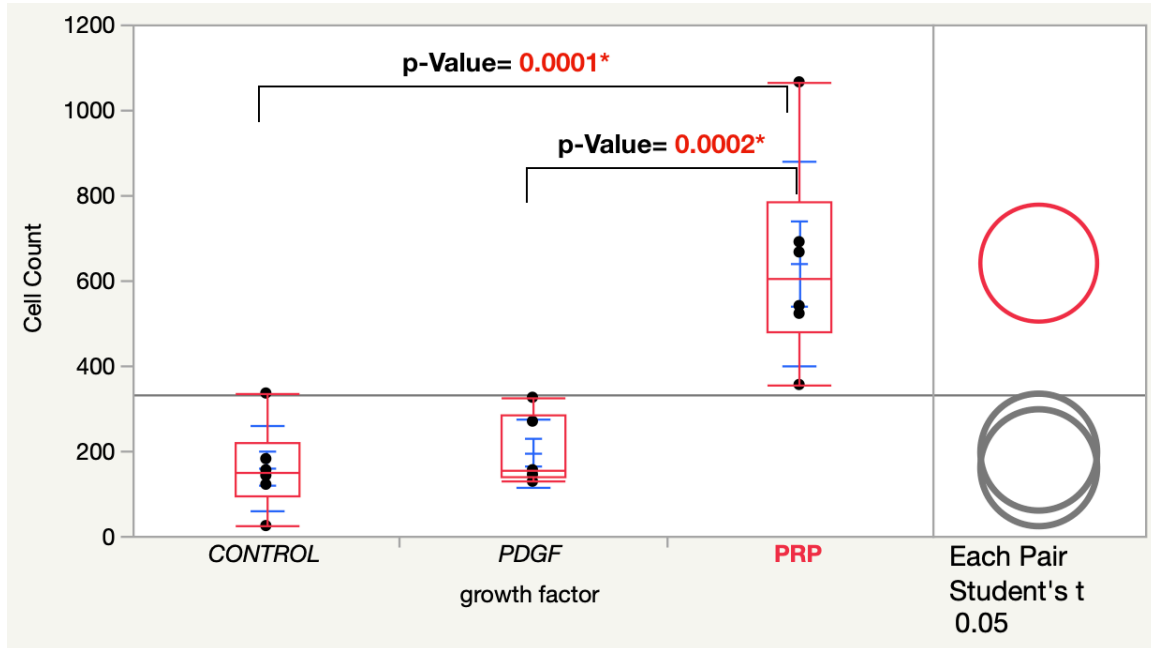


Figure 15. Graph showing pairwise student t-test box plots comparison for each pair of the experimental groups.

Statistical Results removing the outliers:

GROUPS	Sample 1 cell count	Sample 2 cell count	Sample 3 cell count	Sample 4 cell count	Mean	SD
Blank Gtn-HPA	155	142	181	121	149.75	25.1
Gtn-HPA/PDGF-BB	269	157	144	155	226.5	84.55
Gtn-HPA/PRP	522	540	690	666	603	84.35

Table.6. Quantified migrated cells across the collagen ring/Gtn-HPA core interface removing the outliers.

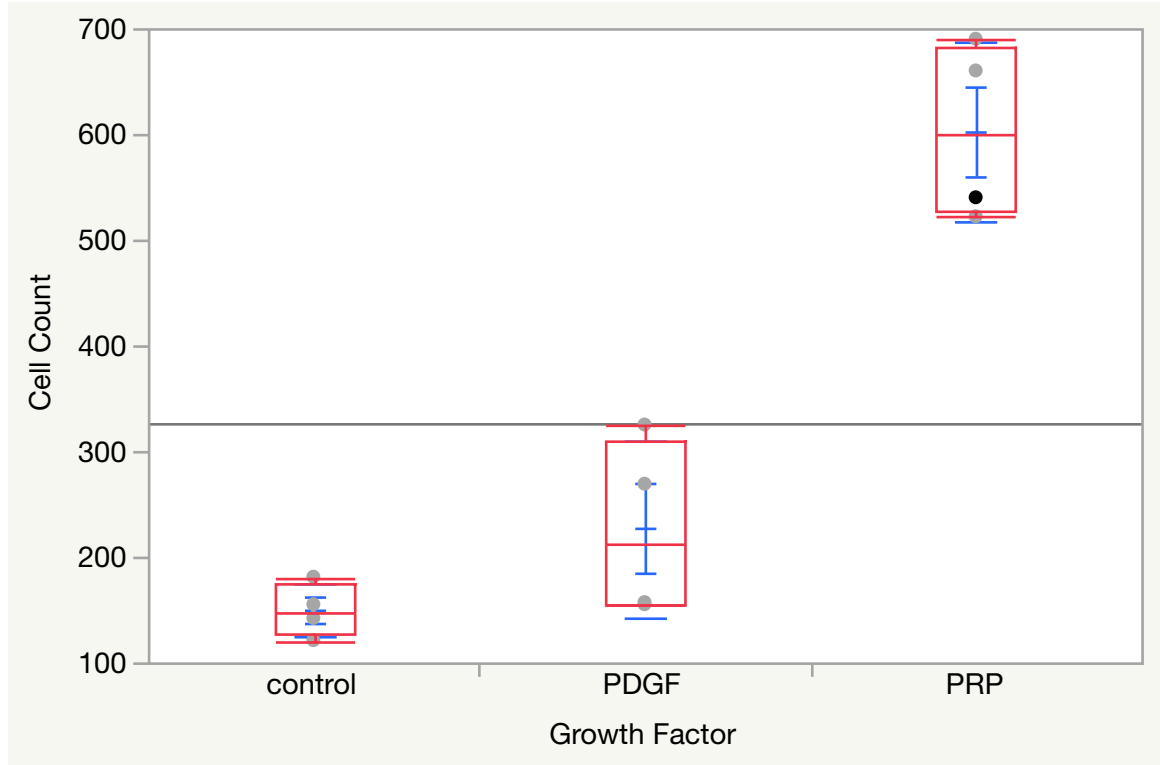


Figure 16. Graph showing one way-ANOVA analysis for migration assay after removing the outliers. P-Value<0.0001*

Gtn-HPA was permissive to osteogenic differentiation, results of the differentiation/osteogenesis assay showed that the area% of osteocalcin+ cells was significantly higher in both the gel/PRP and gel/PDGF-BB groups, compared to the two control groups with cells in the blank gels grown in cell expansion medium and in osteogenic medium.

The Quantitative analysis of the area percentage covered by the Osteocalcin + cells seeded in the hydrogels was significantly higher in the growth factors-infused hydrogels compared to the control groups where either cell expansion medium or osteogenic medium was used as shown in Fig.18 and 19. (One-Way ANOVA and pairwise t-test with P-Value< 0.05). Furthermore, although the Osteogenic medium groups showed osteogenic differentiated cells, the Osterix + cells were more evident than Osteocalcin+ cells as shown in (Figure 17.B)

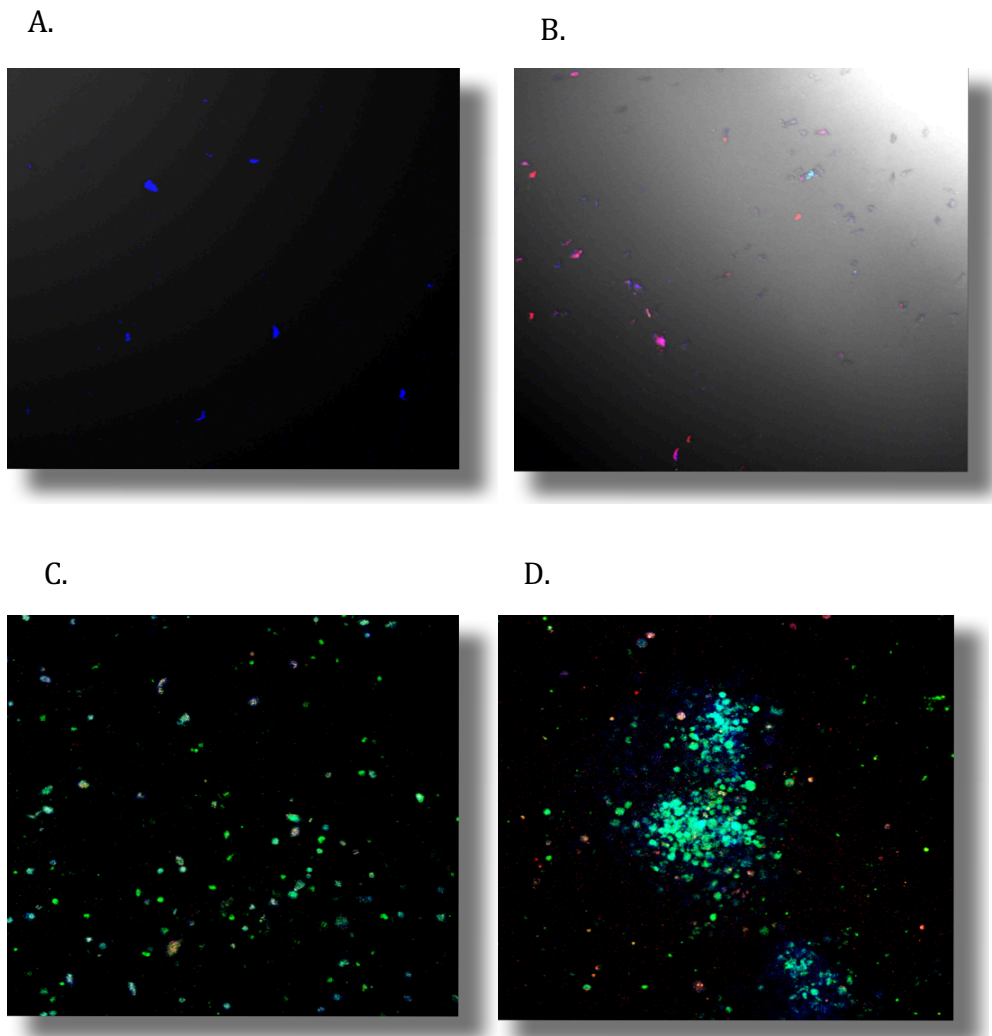


Figure 17. Representative DAPI(Blue)/Anti-Osteocalcin antibody (Green) /Anti-Osterix antibody(Red)- immunostained cells in hydrogel samples for differentiation assay, showing the expression of osteocalcin among the groups. (A)Control with CEM (B) Control group with OM (C)PDGF-BB group (D)PRP-Lysate group

GROUPS	Sample 1 Osteocalcin area%	Sample 2 Osteocalcin area%	Sample 3 Osteocalcin area%	Sample 4 Osteocalcin area%	Sample 5 Osteocalcin area%t	Sample 6 Osteocalcin area%t	Mean	SD
Blank Gtn- HPA/CEM	0%	0%	0%	0%	0%	0%	0	0
Blank Gtn- HPA/OM	0.279%	0.099%	0.019%	0.014%	0.053%	0.133%	0.099	0.09
Gtn- HPA/PDGF- BB/OM	1.687%	6.472%	0.212%	0.478%	0.741%	3.993%	2.26	2.47
Gtn- HPA/PRP/OM	6.37%	1.071%	0.283%	6.465%	0.872%	2.67%	2.955	2.79

Table.7. Showing Image J Results of Quantified Osteocalcin area% among the experimental groups

Differentiation assay Statistical Analysis:

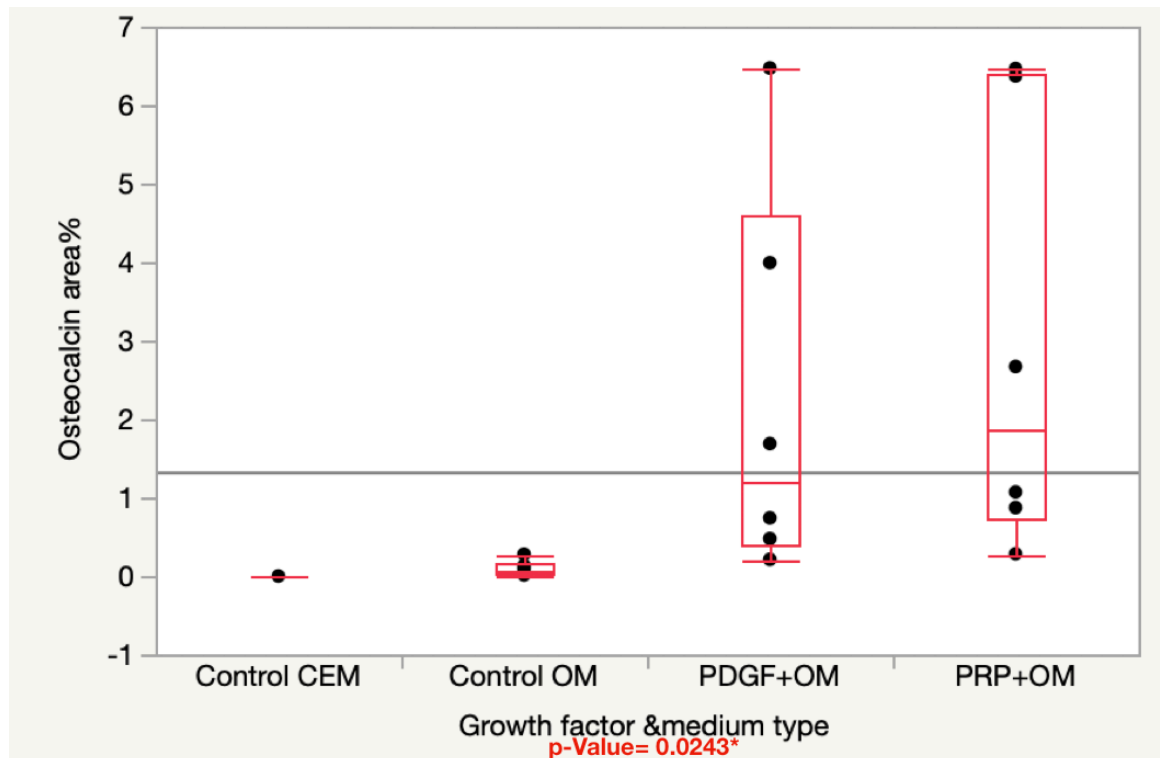


Figure 18. Graph showing one-way ANOVA analysis of Osteocalcin fluorescence area% among the groups

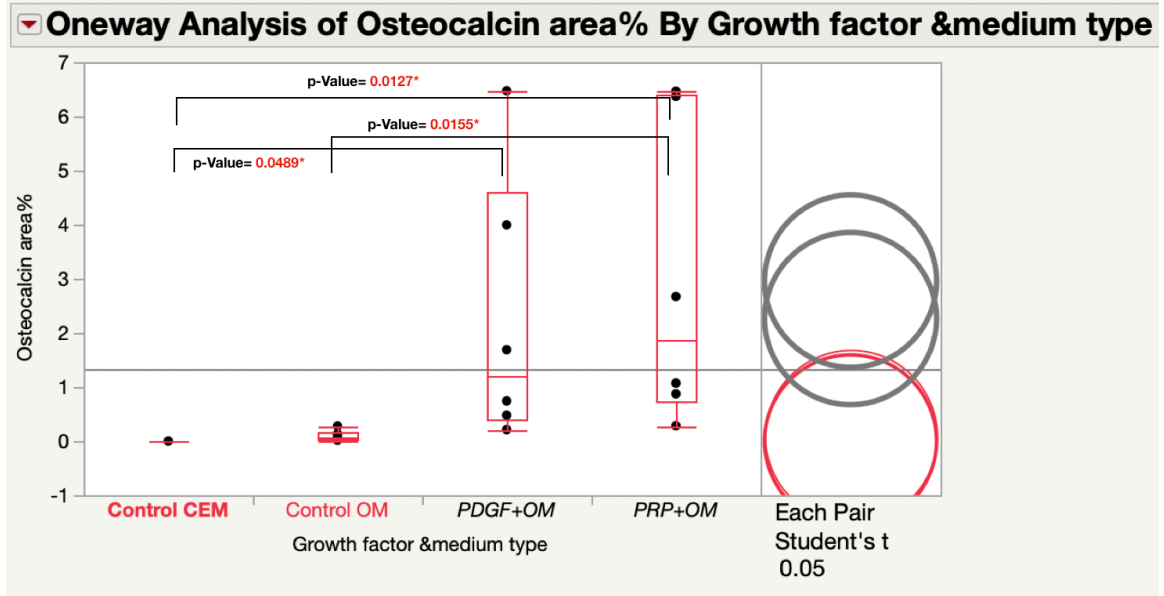


Figure 19. Graph showing one-way analysis of Osteocalcin fluorescence area% among the groups using pairwise student t-test. Significant difference is shown between the two groups using growth factors compared to the two control groups.

The results of the ELISA release assay indicated that Gtn-HPA acted as an effective delivery vehicle for the sustained release of PDGF-BB from 2 different PRP-lysate batches and the pure PDGF-BB group at 28 days

The standards curve fit was calculated using the Four-Parameter logistic regression curve. Afterward, the concentrations of the PDGF and EGF in the collected supernatant at the different time points in then the cumulative release amount were calculated. The results showed that after 28 days, the average of the amount of cumulative released PDGF-BB from PRP Lysate I, PRP Lysate II and the pure PDGF-BB groups were 422.6Pg, 473.5Pg, 440.8Pg respectively. Results also showed that 58%-64%-98.8% of the original PDGF-BB amount remained in the gel at 28 days for the PRP lysate preparations I, II and pure Rat PDGF-BB group. However, there was no statistically significant difference in the cumulative release profile of PDGF-BB among the groups with P value=0.5228. using Fisher’s PLSD statistical analysis for comparison between each pair of the groups also showed no significant differences in the release among them with P-Values as shown in Table [8].

Comparison Groups	Mean Diff.	Crit. Diff.	P-Value
PRPI, PRPII	50.800	95.752	.2702
PRPII, PDGF	32.400	95.752	.4751
PRPI, PDGF	- 18.400	95.752	.6828

Table.8. Showing results of Fisher’s PLSD, Post-hoc Tukey for PDGF release assay among the groups with significance level of 5%

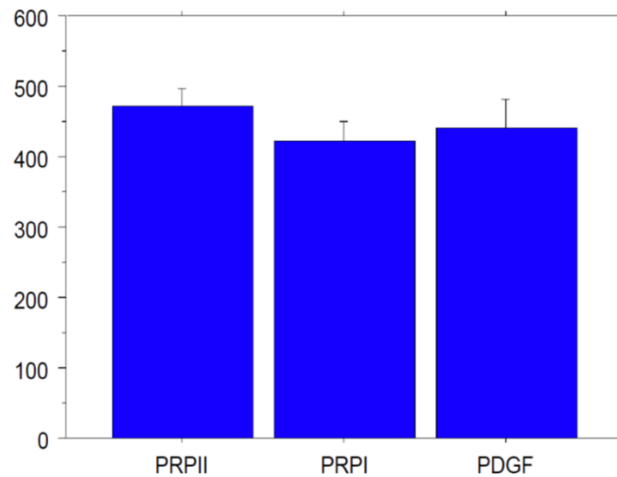


Figure 20. Graph showing no significant difference between the experimental groups for the accumulated release of PDGF from the gelatin-HPA among the groups. One way ANOVA P-Value=0.5228

The results of the ELISA release profile showed no difference between the release of EGF in the 2 PRP-lysate preparations comparison groups.

The amount of EGF quantified in the original two different PRP-Lysate preparations I and II used for the experiment were 4Pg and 3.6Pg respectively. The statistical results of the data showed that there was no significant difference in the cumulative release profile of EGF between the two different PRP-lysate preparations with a P value=0.1910 as shown in table [9]

Comparison Groups	Mean Diff.	DF.	t-value	P-Value
PRPI, PRPII	2.360	8	1.428	.1910

Table.9. Showing Results of t-test for EGF release assay comparison between the two PRP-lysate preparations groups with significance level of 5%.

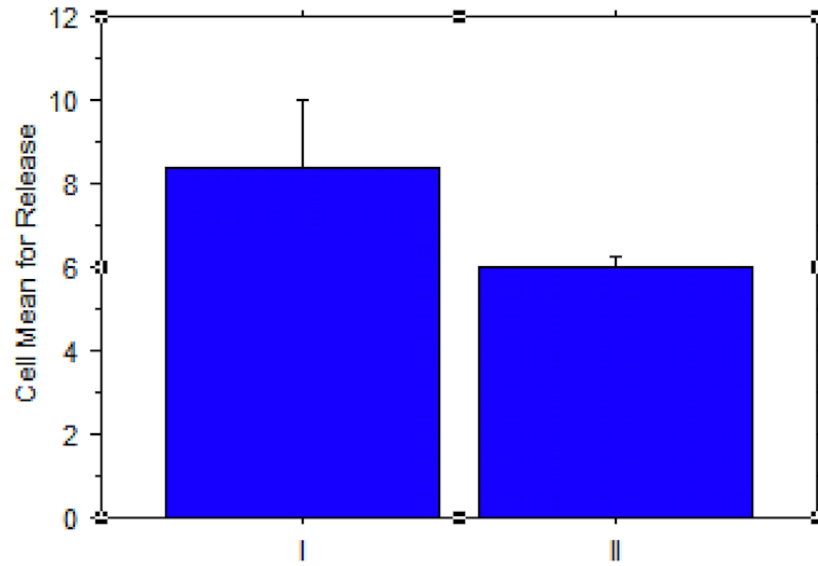


Figure 21. Graph showing no significant difference between the experimental groups for the accumulated release of EGF from the gelatin-HPA among the groups. t-test P-Value=0.1910

Discussion:

Recently for tissue engineering and regenerative medicine, the aim has been leaning towards recruiting the endogenous host progenitor cells to reconstruct and replace the lost tissue. In that sense, attempting to enhance the body's own capacity to repair and regenerate was the goal of this study. In this study, the motivation was that 3D printed porous blocks being heavily studied nowadays for repairing large alveolar bone defects might be necessary but not sufficient for bone regeneration in these large defects. We, therefore, proposed in this study that Gelatin HPA could be used to fill the pores and channels within the 3D printed block. With its covalently cross-linked nano-fibrillar matrix, compared to the fibrin clot that might otherwise fill the 3D printed block, Gelatin HPA can serve as a longer lasting scaffold framework to support cell migration, differentiation, and synthesis of a new matrix. The fibrin clot is not robust enough to fill in large defects thoroughly. The Gtn-HPA can also act as a delivery vehicle for different growth factors sustained release.

What makes Gtn-HPA a particularly promising material for bone regeneration and repair is the wide range of stiffness of the hydrogel which can help in tuning for osteogenic differentiation[36]

It had already been proven previously that cells residing in any scaffold respond differently according to the physical characteristics of these scaffolds. cells may receive different cues that have an impact on cell behavior either in vivo or in vitro.

[30],[27],[36]

Therefore Gtn-HPA with its tunable crosslinking density, degradation rate, and mechanical properties was chosen to be studied in this research for future clinical applicability.

Among the diverse options available nowadays for alveolar bone grafting procedures, autologous bone grafts are the sole scaffold that has the osteoinductive properties. Using the different tools available in tissue engineering might help in developing a scaffold that has the osteoinduction properties mimicking autologous bone grafts. Here in our study, we investigated two principles of osteoinduction. The first one was the chemoattractant ability of the scaffold in recruiting cells towards the defect area. The second principle was to prove that cells migrated into the scaffold will be able to differentiate to prepare for the synthesis of a new matrix in the scaffold. For this in-vitro study 2% Gtn-HPA gel was chosen for all groups.

Our study results showed the permissibility of Gtn-HPA to rat-MSCs cell migration, that was in line with the results of a previous study by Lim et al. [32] using adult neural stem cells (aNSCs), it was concluded that aNSCs were able to migrate into Gtn-HPA gel in a pattern called chain migrations, although the same pattern was shown in our results. PRP lysate infused Gtn-HPA group showed a more extensive interconnected tree like migration into the core hydrogel that was evident with the aSMA staining of the cell's cytoskeleton (Fig.11,13).

Our results from the Ring/Core migration assay showed that PRP-Lysate infused hydrogels showed a significantly higher number of migrating cells compared to control and PDGF-BB groups with a P-Value=0.0001*.

Although it's known and shown in a great body of literature that PDGF-BB is a potent chemoattractant and mitogen for many cell types such as mesenchymal stem cells, osteoblasts, smooth muscle cells, and others, in our study for the migration assay of the rat-MSCs, PDGF unexpectedly showed no significant difference compared to the control group and significantly had less chemoattractant effect compared to the PRP-lysate group.

A pilot study for a migration assay before the main experiment we did was first performed with N=2 per experimental group. In that preliminary study, the results were also similar to our reported final results (Fig25). Although in that preliminary study human PDGF-BB was used at a concentration of 20ng/ml as shown in the appendix page 54. We hypothesized that using the human PDGF-BB or the concentration used might be the reason why there wasn't much migration of the rat MSCs cells in the PDGF group, However, final results showed the same pattern even with using recombinant rat-PDGF at increased concentration 50 ng/ml.

One of the possibilities that might explain this finding is that the rat-MSCs had higher affinity to PRP compared to PDGF. Another possibility can be that the mechanism by which the PDGF is acting on the Rat-MSCs to induce migration is different than the PRP-lysate, so it might have needed more time to take effect. One Intriguing concept that we proposed here that was supported by previous evidence in the literature and gives a stronger explanation is the cross talk between different growth factors that sometimes can be inhibitory.

Previous studies reported the direct interaction between FGF-2 and PDGF-BB and their reciprocal inhibitory effect on different cell types functions. It was reported by Facchiano et al. in their study that FGF-b (FGF-2) had inhibited the chemotactic and mitogenic effect of PDGF on rat aorta smooth muscle cells.[37] In our study, during cell culture and different passaging, FGF-2 was supplemented to the medium to help grow the cells. We believe that this might be one of the possible reasons why the PDGF-BB group didn't show the usual significant higher chemoattractant effect compared to the control group.

Another study by Faraone et al. [38] strongly supported the evidence of cross-talk between the two growth factors. They concluded that PDGF-BB has a reciprocal inhibitory effect on the mitogenic and other FGF-2 induced cell processes of human umbilical vein endothelial cells (HUVECs) by acting on the membrane level.

Although some studies failed to prove a significant improvement in cellular activities or regeneration using PRP-lysate in tissue engineering applications, many other studies showed it had a positive effect. Conclusions aren't made yet and it is still controversial in the current literature due to the heterogeneity of many aspects such as the preparation methods of PRP lysates. In our study PRP-lysate experimental groups showed significantly improved impact of PRP on rat MSCs migration and osteogenic differentiation compared to the control groups. These findings are supported by many other previous studies, Kaduko et al. studied the use of platelet-rich plasma combined with gelatin hydrogel granules and its effect on angiogenesis in murine subcutis. They found that subcutaneous PRP and gelatin hydrogel granules significantly improved angiogenesis compared to control groups and concluded that this combination can be a promising potential treatment adjunct for ischemic disorders.[39]

Another study by Matsui et al.[40] showed the enhanced angiogenic effect by multiple release of PRP contents and basic fibroblast growth factor from gelatin hydrogels. We, therefore, believe that PRP-lysate is a cost-effective autologous source of growth factors which holds a great promise for improving cellular functions and host regenerative ability.

One of the significant cell processes that needed to be investigated in this study, in order to pave the way for the use of the gelatin HPA hydrogel in oral implantology as a scaffold for bone reconstruction was the permissibility of the gel to cell differentiation into osteogenic cells. The results of the differentiation assay showed a significant positive impact of PRP-lysate infused hydrogel and the PDGF-BB group compared to both the control groups with $P=0.0243$.

Two osteogenic markers of interest were selected for staining the samples. The first was Osteocalcin being the main marker of interest in our study. The second marker was the anti-osterix antibody. Osterix is considered an early osteoblastic differentiation maker while Osteocalcin is considered a later osteoblast differentiation marker for mature osteoblasts.[41],[42].

Our results from the differentiation assay based on osteocalcin area% for the one factor-ANOVA showed significant difference with $P\text{-Value}=0.0243$ (Fig.18). The pairwise t-test between each pair of the experimental groups also showed a significant higher osteocalcin + area percentage the PDGF-BB or PRP-lysate infused gelatin-HPA was used compared to both control groups where either cell expansion medium was or osteogenic medium was used (Fig.19)

Although the osteogenic medium group showed both Osterix + and Osteocalcin+ cells. The Osterix fluorescence was more evident than osteocalcin. One possible explanation for the significant difference between this group and the growth factors groups can be that a longer time period was required for it to express osteocalcin which is a late osteogenic marker. However, this group expressed Osterix fluorescence which means the rat MSCs were able to differentiate into pre-Osteoblasts.

Among the different growth factors mentioned in the literature in the field of bone tissue engineering are BMPs, PDGF-BB, and PRP. [41] according to the ELISA growth factor release assay in our study, it can be concluded that Gtn-HPA acted as a delivery vehicle for the sustained release of growth factors over an extended period of time.

One finding of interest in our study was that the release profile for the PDGF-BB from the Gtn-HPA infused with the two different PRP-lysate preparations or the pure PDGF group showed no statistically significant difference among the groups.

These findings indicated that the concentration of growth factor used to infuse the Gtn-HPA hydrogel that was either used as the pure recombinant PDGF-BB or the PDGF in the PRP-lysate didn't affect the concentration or amount of growth factor released from the hydrogel after 28 days. This can support the use of PRP-lysate as an autologous source of growth factors.

One of the other growth factors present in the PRP-Lysate that's known for its mitogenic, osteogenic potential in bone tissue engineering and implant dentistry is EGF. [43]. That's why we assessed the release profile of EGF from 2 different PRP-Lysate preparations in this study, the ELISA results of its release from the Gtn-HPA from the two different PRP-lysate preparations was in line with our PDGF release results. There was also no significant difference in the release profile between both groups.

One factor that's known from previous studies to play a role in the burst release effect of EGF is the size of the growth factor. EGF has a small molecular weight relative to other growth factors. Compared to the 25-30 kDa dimer PDGF, EGF is only a 6kDa one [44]

One more thing in this study that might have contributed to the fast diffusion of EGF from the hydrogel was the low cross-linking density of the 2% Gtn-HPA hydrogel. Nonetheless, for the EGF release results, no definitive conclusion can be drawn because of the low amount of EGF present in the original PRP-Lysate preparations used, which was as little as ~4Pg.

On another note, in a study done in our laboratory by Shah Adhvait, on the release of EGF from different Gtn-HPA densities, 8%, and 12%, EGF was still present in the gel after 4 weeks, confirming that Gtn-HPA acted as a delivery vehicle for sustained release.

In the future, using a higher concentration of a recombinant EGF group can be included, similar to the PDGF study, in order to assess the sustained release of EGF, but it was proven in our lab in a different study.

Future directions and preliminary qualitative assessment results for experiments with 3D printed blocks:



Figure 22. showing photos for the 3D printed porous calcium phosphate(CaP) block on the left, and the Gelatin-HPA Infused (CaP) 3D printed blocks.

3D Printed blocks migration assay used for preliminary data analysis:

Sample grouping: N=6

- 1) **Group 1 “Control group”:** Blank Gtn-HPA infused 3D printed blocks
- 2) **Group 2:** PRP-lysate incorporated Gtn-HPA infused 3D printed blocks

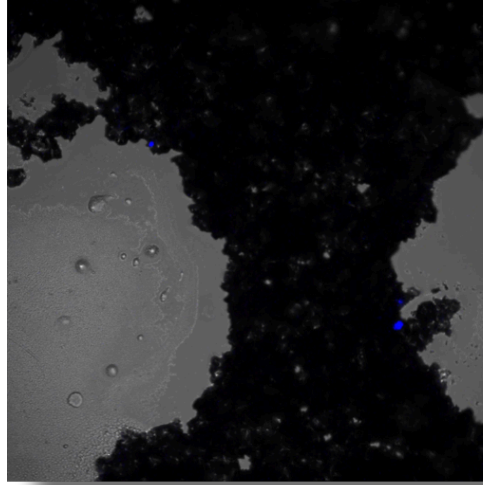
Pre-staining method for 3D printed Blocks:

Many methods were tried to find the best way to visualize and examine the cell migration and osteogenesis in the Gtn-HPA infused 3D porous calcium-phosphate histologically. For the preliminary study, however, there were several obstacles. The regular H&E staining and the alternative multiple stain MSS solution of the non-decalcified sections resulted in poor quality images. Because of the thick thickness of the sections which had to be at least 60μ to maintain the integrity of the block. The other problem was the debonding of the sections from the slide sometimes was noted for the same reason. After many trials, in this study a solution trying a different method worked. Immuno-prestaining the blocks and then using frozen section histology that was later examined using confocal microscopy. This method proved to work and images were obtained shown in (Fig.23) for the qualitative assessment of the preliminary migration assay using the 3D printed blocks.

Preliminary Results for the 3D printed blocks migration assay:

Results of the qualitative assessment of the confocal images are showing more migration into the pores and channels of the PRP-Lysate infused 3D printed blocks compared to the blank hydrogel infused 3D printed blocks as seen in (Fig.23).

A.



B.

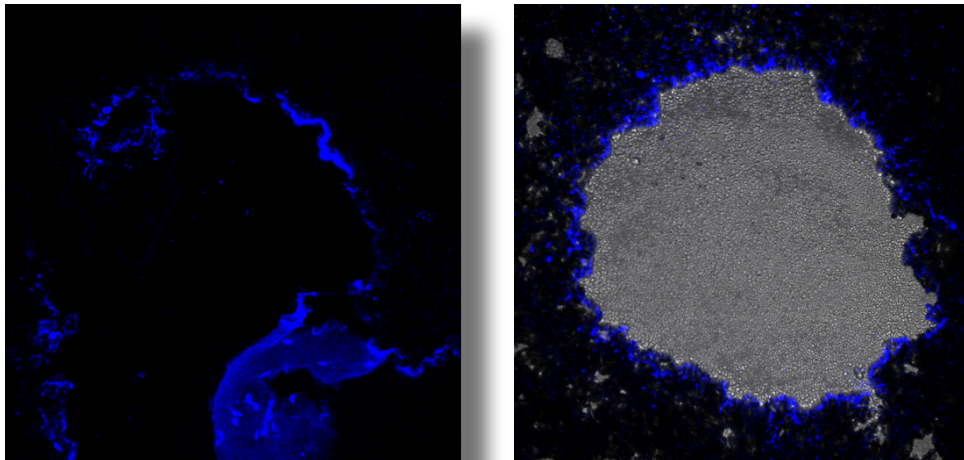


Figure 23. Confocal microscopy images for the qualitative assessment for the blocks migration assay. Showing Dapi-stained nuclei of migrated cells into the 3D printed calcium phosphate blocks after 10 days. Pre-immunostaining method described in page 58. (a) Control group with the 3D printed block infused with the blank hydrogel (b) PRP-Lysate group with the prp-lysate infused 3D printed block
DAPI Prestaining method for the 3D printing blocks:
cryosections were 100micron thickness, examined using Confocal Microscopy.

Results of the qualitative assessment of the confocal images are showing more migration into the pores and channels of the PRP-Lysate infused 3D printed blocks compared to the blank hydrogel infused 3D printed blocks as seen in (Fig.22).

Conclusions:

Based on our findings it was concluded that the results of the *in vitro* experiments supported our 3 hypotheses regarding the utility of Gtn-HPA for bone reconstruction. The data showed that Gtn-HPA was permissive of cell migration. PRP-lysate infused hydrogels displayed increased rat MSC migration into the Gtn-HPA compared to the blank gel and the PDGF-BB containing hydrogel. Regarding the differentiation/osteogenesis assay, the PRP-lysate and the PDGF-BB incorporating gel showed a greater area% of osteocalcin+ cells compared to the blank gel containing hydrogel. The release of the growth factors from PRP lysate, incorporated onto the gel, extended over the period of time necessary for bone reconstruction.

These findings commend Gtn-HPA incorporating PRP-lysate for infusion into porous calcium phosphate blocks for vertical and horizontal ridge reconstruction. This scaffold biomaterial can be considered as a new category of scaffolds which not only has a cell accommodative nature but also can act as a delivery vehicle for different regulators by incorporating them to optimize tissue reconstruction and host regenerative capacity. Hence, becoming a scaffold that has osteoinductive properties mimicking autologous grafts.

Appendix:

I. Migration assay pilot experiment using 20ng human PDGF-BB “N=2”

Experimental groups were divided as follows:

Group 1: “control group” in which the blank Gtn-HPA hydrogel

Group 2: PRP lysate infused Gtn-HPA hydrogel

Group 3: Pure recombinant PDGF-BB infused Gtn-HPA hydroge

Results from this experiment showed the same results in terms of that there was also no significant difference

GROUPS	Sample 1 cell count	Sample 2 cell count	Mean	SD
Blank Gtn-HPA	34	74	54	28.28
Gtn-HPA/PDGF-BB	70	36	53	24.04
Gtn-HPA/PRP	472	300	386	121.6

Table.10. Showing the migration assay cell count, means and standard deviations among the experimental different groups

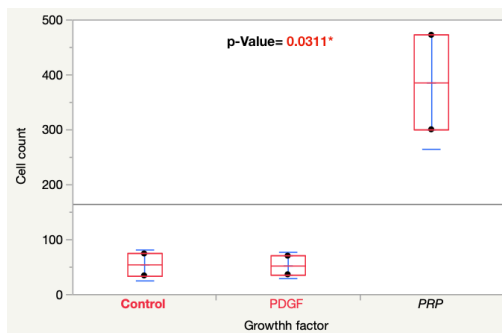


Figure 24. Graph showing one way Anova Boxplots for the migration assay.
P-value=0.0311*

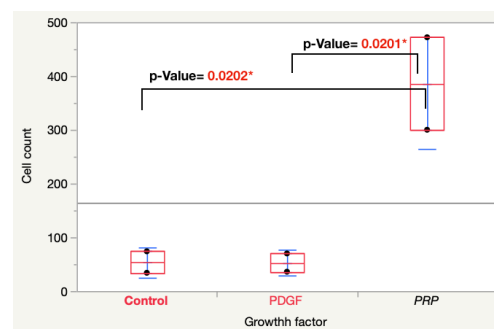


Figure 25. Graph showing pairwise t-test between each pair of the experimental groups with the significant P-values shown on the figure.

II. MMA 3D printed BLOCK EMBEDDING “Based on Dr.Ronald Baron’s Lab at HSDM”

For the base bed preparation:

1. Prepare 85% of the MMA solution “850ml” + 15% “150ml” of the Dibutyl Phalate +3% benzoyl peroxide “30mg”
2. Put a stirrer in the beaker and stir the soln. for 4 hours
3. We added the embedding solution with the electric pipette in the chemical hood
in each of the vials-the vials used as the mold for the block embedding-was set in the vacuum desiccator.
4. Then we took the tubes to the oven, left them at 58° Celsius for overnight.

Different Infiltration Solutions used for MMA embedding:

- **Infiltration Solution #1:**
Mix 85% of MMA solution + 15% Dibutyl Phalate
stir for 4 hours at 4°C, keep stored at the same temperature
- **Infiltration Solution#2:**
Mix 85% of MMA solution + 15% Dibutyl Phalate +0.1% Benzoyl peroxide
Stir for 4 hours at 4°C, then store at 4°C
- **Infiltration Solution#3:**
Mix 85%MMA + 15% Dibutyl Phalate +3% Benzoyl peroxide
Stir for 4 hours, store in 4°C
- **MMA Embedding solution:**
it should be freshly prepared on the same day of embedding
Mix 85%MMA + 15%Dibutyl Phalate + 3% Benzoyl Peroxide
Stir for 4 hours at 4°C.

For the 3D printed block in this study:

1. **Fixation Step:**
all fixations are done at 4°C:
 - The block is immersed in 70% alcohol replacing it daily 3 times
 - Day 4 block is placed in acetone.
2. **Day 5:**
After removal of Acetone, the block was placed in the infiltration solution #1 from for 5 days at 4° Celsius in a vacuum desiccator.
3. **Day 10:**

Let the Vacuum Desiccator warm up from 4°C to room temperature

for at least 2 hours

Pour out infiltration solution#1, then add 8ml of infiltration solution#2. In the vacuum desiccator at 4°C for 5 days

4. **Day 15:**

Let the vacuum desiccator warm up from 4°C to room temperature for at least 2 hours.

Pour out infiltration solution#2, then add 8ml of infiltration solution#3. In the vacuum desiccator at 4°C for 5 days.

5. **Day 20:**

Let the vacuum desiccator warm up from 4°C to room temperature for at least 2 hours.

After preparing the fresh embedding solution, add 8ml of it to the base prepared before and leave it in the oven 37°C for 30 minutes to soften the base for better orientation of the block.

leave it to polymerize for 3 days.

6. **Once Polymerized:**

Leave the vial in -20°C for 15 minutes, then hammer break the glass to take out the polymerized block

MMA Block was then ground to a suitable size using (Buehler MetaServ'3000 Grinder and polisher) and trimmed to 60µ slice using (Leica RM2255 machine with 16cm/D blade). The sample was then glued on slides.

add 2-3 drops of 20% Ethoxy-Ethyl acetate mixed with 70% alcohol on the section. Cover section with plastic film. Then squeeze out the liquid gently and clamp the slides with a big metal binder clip and leave it in 37°C for 4 days. After that, the slides are ready for staining.

**Block Sectioning:
sectioning was done using Leica**

The calcium phosphate sectioning was challenging because of the slice sections that wouldn't compromise the integrity of the block. After many trials, it was found that the minimum thickness that was obtained with sound integrity of the block was 50-60-micron section thickness.

III. **Block Slides Staining**

- **For the H&E Staining that worked:**

1. Place the slide in 100% Ethanol & EOSIN For 5 minutes
2. Then in xylene for 3 minutes
3. Filter the hematoxylin, then put the slide in hematoxylin for 5 minutes
4. Place the slide in Xylene for 2 minutes and 30 sec.

- **For the Multiple Stain Solution "MSS":**

1. Using a small plastic pipette, add the MSS solution directly to the slide; stain for 30 seconds
2. Rinse carefully in gently running tap water
3. Dehydrate very quickly in 95% ethanol bath twice
4. Then in 100% ethanol
5. Then in xylene twice
6. Coverslip with poly-mount mounting media as quickly as possible

IV. **The pre-straining method that gave the best quality images:**

1. After fixation of the cells 10 days after the migration assay ended. Samples were fixed by adding 1ml of 4% PFA in each well and was left overnight.
2. PFA was then removed, 1ml of PBS treated with 0.1% triton X100 was added to each sample and left for 2 hours
3. Triton was removed then samples were washed by adding 1ml of PBS, left for 30 minutes.
4. Dako protein block serum-free (Abcam, USA) was added to each sample. samples were left in the refrigerator for the next day.
5. Primary and secondary antibody staining was used as described earlier in the study.
6. Dapi staining as well was left for 24 hours before frozen section steps were started.

V. **Frozen sectioning:**

After embedding the block in OCT medium for overnight, same protocol of frozen sections was followed, keeping the blocks in -80°C for an overnight before sectioning. Sections were 100µ thick.

List of Figures:

Figure 1. Schematic diagram representing inflammatory and repair events in the bone healing process after tooth extraction.

Figure 2. Diagram showing the tissue engineering triad. Gelatin-HPA scaffold in our study representing combinatorial treatment modality allowing the interplay of different Tissue Engineering tools

Figure 3. Diagram showing platelets originating from blood vessel injury and their mother cell in the bone marrow

Figure 4. Cultured Rat-MSCs cell-lineage differentiation

Figure 5. Diagram showing the processing method performed in our lab to obtain PRP-Lysate

Figure 6. Schematic Drawing for the two-step fabrication of Gtn-HPA gel

Figure 7. Photo of the migration assay sample showing the Collagen Ring and the core Gtn-HPA

Figure 8. Diagram showing the sample grouping for the migration assay and their respective growth factors concentrations used migration assay ..sample showing the Collagen Ring and the core Gtn-HPA

Figure 9. Nikon Eclipse C2+ laser scanning system confocal microscopy used for imaging

Figure 10. Superimposed Image of one of the samples showing the DAPI stained nuclei image superimposed on the Bright field confocal microscopy image

Figure 11. Confocal microscopy images using 10x Macro objective lens. Showing double staining DAPI/Anti α SMA elucidating the pattern of migration of the rat-MSCs from the collagen ring into the Gtn-HPA core hydrogel.

Figure 12. Showing a sample of the cell-seeded gelatin-HPA hydrogel casted in the well of 48-well cell culture plate.

Figure 13. Representative DAPI(Blue)/Anti α - SMA(Green) immunostained hydrogels, showing the Ring/Core interface and the migrating rat-MSCs into the core Gtn-HPA for the experimental groups.

Figure 14. Graph showing one way-ANOVA analysis for the migration assay "Cell Count" by "Growth Factor" among the groups

Figure 15. Graph showing pairwise student t-test box plots comparison for each pair of the experimental groups

Figure 16. Graph showing one way-ANOVA analysis for migration assay after removing the outliers. P-Value<0.0001*

Figure 17. Representative DAPI(Blue)/Anti-Osteocalcin antibody (Green) /Anti-Osterix antibody(Red)- immunostained cells in hydrogel samples for differentiation assay, showing the expression of osteocalcin among the groups. (A)Control with CEM (B) Control group with OM (C)PDGF-BB group (D)PRP-Lysate group

Figure 18. Graph showing one-way ANOVA analysis of Osteocalcin fluorescence area% among the groups

Figure 19. Graph showing one-way analysis of Osteocalcin fluorescence area% among the groups

using pairwise student t-test. A significant difference is shown between the two groups using growth factors compared to the two control groups.

Figure 20. Figure 20. Graph showing no significant difference between the experimental groups for the accumulated release of PDGF from the gelatin-HPA among the groups.

One-way ANOVA P-Value=0.5228

Figure 21. Graph showing no significant difference between the experimental groups for the accumulated release of EGF from the gelatin-HPA among the groups.

t-test P-Value=0.1910

Figure 22. showing photos for the 3D printed porous calcium phosphate (CaP) block on the left, and the Gelatin-HPA Infused (CaP) 3D printed blocks

Figure 23. Confocal microscopy images for the qualitative assessment for the blocks migration assay. Showing Dapi-stained nuclei of migrated cells into the 3D printed calcium phosphate blocks after 10 days.

Figure 24. Graph showing one-way ANOVA Boxplots for the migration assay. P-value=0.0311*

Figure 25. Graph showing pairwise t-test between each pair of the experimental groups with the significant P-values shown on the figure.

List of Tables

Table.1. Gtn-HPA formulation and the concentrations of the constituents

Table.2. Showing Anti-Osteocalcin Antibody and Anti-SP7/Osterix immunostaining protocol used

Table.3. Showing Experimental groups for PDGF release study with the concentration of gelatin-HPA fabrication constituents.

Table.4. Showing Experimental groups for PDGF release study with the concentration of the Gelatin-HPA fabrication constituents.

Table.5. Quantification of migrated cells across the collagen ring/Gtn-HPA core interface among the different experimental groups. The cell count was done after 10 days of the migration assay based on DAPI stained nuclei using Image J software.

Table.6. Quantified migrated cells across the collagen ring/Gtn-HPA core interface after removing the outliers.

Table.7. Showing Image J Results of Quantified Osteocalcin area% among the experimental groups

Table.8. Showing results of Fisher's PLSD, Post-hoc Tukey for PDGF release assay among the groups with a significance level of 5%

Table.9. Showing Results of t-test for EGF release assay comparison between the two PRP-lysate preparations groups with a significance level of 5%.

Table.10. Showing the migration assay cell count, means and standard deviations among the experimental different group

Bibliography:

1. Chiapasco, M. and P. Casentini, *Horizontal bone-augmentation procedures in implant dentistry: prosthetically guided regeneration*. *Periodontol* 2000, 2018. **77**(1): p. 213-240.
2. Esposito, M., et al., *The efficacy of horizontal and vertical bone augmentation procedures for dental implants - a Cochrane systematic review*. *Eur J Oral Implantol*, 2009. **2**(3): p. 167-84.
3. Urban, I.A.s., et al., *Effectiveness of vertical ridge augmentation interventions. A systematic review and meta-analysis*. *J Clin Periodontol*, 2019.
4. Jung, J.W., J.S. Lee, and D.W. Cho, *Computer-aided multiple-head 3D printing system for printing of heterogeneous organ/tissue constructs*. *Sci Rep*, 2016. **6**: p. 21685.
5. Parthasarathy, J., *3D modeling, custom implants and its future perspectives in craniofacial surgery*. *Ann Maxillofac Surg*, 2014. **4**(1): p. 9-18.
6. Pilipchuk, S.P., et al., *Tissue engineering for bone regeneration and osseointegration in the oral cavity*. *Dent Mater*, 2015. **31**(4): p. 317-38.
7. Meyer-Blaser, U., &Weismann, H., *Bone and cartilage engineering*. Berlin; 2006: New York: Springer.
8. Politis, C., et al., *Wound Healing Problems in the Mouth*. *Front Physiol*, 2016. **7**: p. 507.
9. Pagni, G., et al., *Postextraction alveolar ridge preservation: biological basis and treatments*. *Int J Dent*, 2012. **2012**: p. 151030.
10. Vieira, A.E., et al., *Intramembranous bone healing process subsequent to tooth extraction in mice: micro-computed tomography, histomorphometric and molecular characterization*. *PLoS One*, 2015. **10**(5): p. e0128021.
11. Chappuis, V., M.G. Araujo, and D. Buser, *Clinical relevance of dimensional bone and soft tissue alterations post-extraction in esthetic sites*. *Periodontol* 2000, 2017. **73**(1): p. 73-83.
12. Araujo, M.G. and J. Lindhe, *Dimensional ridge alterations following tooth extraction. An experimental study in the dog*. *J Clin Periodontol*, 2005. **32**(2): p. 212-8.
13. McAllister, B.S. and K. Haghghat, *Bone augmentation techniques*. *J Periodontol*, 2007. **78**(3): p. 377-96.
14. Simion, M., et al., *Vertical ridge augmentation by means of deproteinized bovine bone block and recombinant human platelet-derived growth factor-BB: a histologic study in a dog model*. *Int J Periodontics Restorative Dent*, 2006. **26**(5): p. 415-23.
15. Simion, M., I. Rocchietta, and C. Dellavia, *Three-dimensional ridge augmentation with xenograft and recombinant human platelet-derived growth factor-BB in humans: report of two cases*. *Int J Periodontics Restorative Dent*, 2007. **27**(2): p. 109-15.

16. Rasperini, G., et al., *3D-printed Bioresorbable Scaffold for Periodontal Repair*. J Dent Res, 2015. **94**(9 Suppl): p. 153S-7S.
17. Avila-Ortiz, G., et al., *Biologics and Cell Therapy Tissue Engineering Approaches for the Management of the Edentulous Maxilla: A Systematic Review*. Int J Oral Maxillofac Implants, 2016. **31 Suppl**: p. s121-64.
18. Marx, R.E., *Platelet-rich plasma: evidence to support its use*. J Oral Maxillofac Surg, 2004. **62**(4): p. 489-96.
19. Lee, K., et al., *Bone regeneration via novel macroporous CPC scaffolds in critical-sized cranial defects in rats*. Dent Mater, 2014. **30**(7): p. e199-207.
20. Pocaterra, A., et al., *Effectiveness of platelet-rich plasma as an adjunctive material to bone graft: a systematic review and meta-analysis of randomized controlled clinical trials*. Int J Oral Maxillofac Surg, 2016. **45**(8): p. 1027-34.
21. Filho Cerruti, H., et al., *Allogeneous bone grafts improved by bone marrow stem cells and platelet growth factors: clinical case reports*. Artif Organs, 2007. **31**(4): p. 268-73.
22. Marx, R.E., et al., *rhBMP-2/ACS grafts versus autogenous cancellous marrow grafts in large vertical defects of the maxilla: an unsponsored randomized open-label clinical trial*. Int J Oral Maxillofac Implants, 2013. **28**(5): p. e243-51.
23. Buwalda, S.J., et al., *Hydrogels in a historical perspective: from simple networks to smart materials*. J Control Release, 2014. **190**: p. 254-73.
24. Lee, S.C., I.K. Kwon, and K. Park, *Hydrogels for delivery of bioactive agents: a historical perspective*. Adv Drug Deliv Rev, 2013. **65**(1): p. 17-20.
25. Buwalda, S.J., T. Vermonden, and W.E. Hennink, *Hydrogels for Therapeutic Delivery: Current Developments and Future Directions*. Biomacromolecules, 2017. **18**(2): p. 316-330.
26. Sakai, S., et al., *An injectable, in situ enzymatically gellable, gelatin derivative for drug delivery and tissue engineering*. Biomaterials, 2009. **30**(20): p. 3371-7.
27. Wang, L.S., et al., *The role of stiffness of gelatin-hydroxyphenylpropionic acid hydrogels formed by enzyme-mediated crosslinking on the differentiation of human mesenchymal stem cell*. Biomaterials, 2010. **31**(33): p. 8608-16.
28. Lim, T.C., et al., *The effect of injectable gelatin-hydroxyphenylpropionic acid hydrogel matrices on the proliferation, migration, differentiation and oxidative stress resistance of adult neural stem cells*. Biomaterials, 2012. **33**(12): p. 3446-55.
29. Lee, F., K.H. Bae, and M. Kurisawa, *Injectable hydrogel systems crosslinked by horseradish peroxidase*. Biomed Mater, 2015. **11**(1): p. 014101.
30. Wang, L.S., et al., *Modulation of chondrocyte functions and stiffness-dependent cartilage repair using an injectable enzymatically crosslinked hydrogel with tunable mechanical properties*. Biomaterials, 2014. **35**(7): p. 2207-17.
31. Chun, Y.Y., et al., *A Periosteum-Inspired 3D Hydrogel-Bioceramic Composite for Enhanced Bone Regeneration*. Macromol Biosci, 2016. **16**(2): p. 276-87.
32. Lim, T.C., et al., *Chemotactic recruitment of adult neural progenitor cells into multifunctional hydrogels providing sustained SDF-1alpha release and compatible structural support*. FASEB J, 2013. **27**(3): p. 1023-33.

33. Huang, S., et al., *An improved protocol for isolation and culture of mesenchymal stem cells from mouse bone marrow*. J Orthop Translat, 2015. **3**(1): p. 26-33.
34. Textor, J.A. and F. Tablin, *Activation of equine platelet-rich plasma: comparison of methods and characterization of equine autologous thrombin*. Vet Surg, 2012. **41**(7): p. 784-94.
35. Wang, L.S., et al., *Injectable biodegradable hydrogels with tunable mechanical properties for the stimulation of neurogenesis differentiation of human mesenchymal stem cells in 3D culture*. Biomaterials, 2010. **31**(6): p. 1148-57.
36. Wang, L.S., et al., *Enzymatically cross-linked gelatin-phenol hydrogels with a broader stiffness range for osteogenic differentiation of human mesenchymal stem cells*. Acta Biomater, 2012. **8**(5): p. 1826-37.
37. Facchiano, A., et al., *The chemotactic and mitogenic effects of platelet-derived growth factor-BB on rat aorta smooth muscle cells are inhibited by basic fibroblast growth factor*. J Cell Sci, 2000. **113 (Pt 16)**: p. 2855-63.
38. Faraone, D., et al., *Heterodimerization of FGF-receptor 1 and PDGF-receptor-alpha: a novel mechanism underlying the inhibitory effect of PDGF-BB on FGF-2 in human cells*. Blood, 2006. **107**(5): p. 1896-902.
39. Kakudo, N., et al., *Angiogenic effect of platelet-rich plasma combined with gelatin hydrogel granules injected into murine subcutis*. J Tissue Eng Regen Med, 2017. **11**(7): p. 1941-1948.
40. Matsui, M. and Y. Tabata, *Enhanced angiogenesis by multiple release of platelet-rich plasma contents and basic fibroblast growth factor from gelatin hydrogels*. Acta Biomater, 2012. **8**(5): p. 1792-801.
41. Miron, R.J. and Y.F. Zhang, *Osteoinduction: a review of old concepts with new standards*. J Dent Res, 2012. **91**(8): p. 736-44.
42. Wagner, E.R., et al., *Therapeutic Implications of PPARgamma in Human Osteosarcoma*. PPAR Res, 2010. **2010**: p. 956427.
43. Del Angel-Mosqueda, C., et al., *Epidermal growth factor enhances osteogenic differentiation of dental pulp stem cells in vitro*. Head Face Med, 2015. **11**: p. 29.
44. Dunn, I.F., O. Heese, and P.M. Black, *Growth factors in glioma angiogenesis: FGFs, PDGF, EGF, and TGFs*. J Neurooncol, 2000. **50**(1-2): p. 121-37.

